Enhancement of antitumor natural killer cell activation by orally administered Spirulina extract in mice

Yuusuke Akao,[1,6] Takashi Ebihara,[1,6] Hisayo Masuda,[2,5,6] Yoshiko Saeki,[2] Takashi Akazawa,[2] Kaoru Hazeki,[3] Osamu Hazeki,[3] Misako Matsumoto[1,2] and Tsukasa Seya[1,2,4]

[1]Department of Microbiology and Immunology, Hokkaido University Graduate School of Medicine, Kita-15, Nishi-7, Kita-ku Sapporo 060-8638; [2]Department of Immunology, Osaka Medical Center for Cancer, Nakamichi 1-3-2, Higashinari-ku, Osaka 537-8511; [3]The Division of Molecular Medical Science, Graduate School of Biomedical Sciences, Hiroshima University, Minami-ku, Hiroshima 734-8551, Japan

(Received October 27, 2008/Revised April 6, 2009/Accepted April 8, 2009/Online publication May 6, 2009)

Oral administration of hot-water extract of Spirulina, cyanobacterium *Spirulina platensis*, leads to augmentation of NK cytotoxicity in humans. Here, we applied to syngeneic tumor-implant mice (C57BL/6 *versus* B16 melanoma) Spirulina to elucidate the mechanism of raising antitumor NK activation. A B16D8 subcell line barely expressed MHC class I but about 50% expressed Rae-1, a ligand for NK activation receptor NKG2D. The Rae-1-positive population of implant B16 melanoma was effectively eliminated in the tumor mass progressed in mice. This antitumor activity was induced in parallel with IFN-γ and abolished in mice by treatment with asialoGM-1 but not CD8β Ab, suggesting the effector is NK cell. NK cell activation occurred in the spleen of wild-type mice medicated with Spirulina. This Spirulina-mediated enhanced NK activation was abrogated in MyD88 –/– mice but not in TICAM-1 –/– mice. The NK activating properties of Spirulina depending on MyD88 were confirmed with *in vitro* bone marrow-derived dendritic cells expressing TLR2/4. In D16D8 tumor challenge studies, the antitumor effect of Spirulina was abolished in MyD88 –/– mice. Hence, orally administered Spirulina enhances tumoricidal NK activation through the MyD88 pathway. Spirulina exerted a synergistic antitumor activity with BCG–cell wall skeleton, which is known to activate the MyD88 pathway via TLR2/4 with no NK enhancing activity. Spirulina and BCG–cell wall skeleton synergistically augmented IFN-γ production and antitumor potential in the B16D8 *versus* C57BL/6 system. We infer from these results that NK activation by Spirulina has some advantage in combinational use with BCG–cell wall skeleton for developing adjuvant-based antitumor immunotherapy. (*Cancer Sci* 2009; 100: 1494–1501)

The immune system has innate and acquired arms to eliminate foreign cells from the host. The innate system recognizes pathogenic microbes which possess pattern molecules serving as ligands for pattern-recognition receptors.[1] These receptors reside in immune competent cells and trigger signaling to activate transcription factors in these cells.[2] Many cytokines and cellular effectors are consequently induced to orchestrate host defense. We have a variety of foods that may contain many kinds of microbial patterns. Since intestinal and colon epithelial cells express pattern-recognition receptors,[3,4] mucosal immune responses may be modulated by oral uptake of microbial material.

The cyanobacterium *Spirulina platensis* (Spirulina) has been taken as a supplemental food for more than 15 years without any undesirable side-effects.[5] Its safety for human consumption has been confirmed through toxicological studies.[5] Spirulina contains a lipopolysaccharide (LPS)-like constituent that structurally differs from the bacterial LPS.[6] Spirulina also contains high contents of protein, vitamins (especially A and B12) and minerals. It is rich in phenolic acids, tocopherols and γ-linolenic acid.[5,7] Since Spirulina lacks cell walls, it is easily digested.[7] Spirulina contains unique proteins, sugars and lipids[5,8] and these moieties of Spirulina are reported to participate in raising host immune responses including enhancement of Ab production,[9] cytokine liberation,[10] T-cell response and NK activation.[11] However, the exact molecular base responsible for these immune responses has not been clearly identified yet.

We previously reported that hot-water extract of Spirulina when taken orally in adult human enhances NK activation.[11] This Spirulina activity is unique since most of the reported bacterial adjuvants facilitate CTL induction but not NK activation.[12] For example, BCG–cell wall skeleton (CWS) subcutaneously injected induces IL-12, IFN-γ and local skin erosion but no NK activation.[13] TLR2 and TLR4 on myeloid dendritic cells (DCs) sense the peptidoglycan (PGN) of BCG (BCG–PGN) and induces DC maturation via the MyD88 pathway.[13,14] BCG–PGN drives DCs to elicit a CTL-inducing state.[15]

Here we show that hot-water extract of Spirulina activates NK in mice even by oral administration. Ingestion of Spirulina confers both IFN-γ production and NK-mediated Rae-1-positive cell killing activity in mice. Consequently, Spirulina administration leads to retardation of implant tumor growth in mice. This Spirulina antitumor activity depends on MyD88 but not the other adaptor TICAM-1 (TRIF). Thus, Spirulina evokes a unique MyD88-dependent NK activation through mucosal immune responses. We offer a possible immune therapy of BCG–CWS in combination with Spirulina in this communication.

Materials and Methods

Reagents and antibodies. The following materials were obtained: fetal calf serum (FCS) from Bio Whittaker (Walkersville, MD), mouse granulocyte–macrophage colony-stimulating factor (GM-CSF) and mouse IL-2 (mIL-2) from PeproTech EC, Ltd (London, UK), polymyxin B and lipopolysaccharide (LPS) (*Escherichia coli* O111:B4) from Sigma-Aldrich (St. Louis, MO), synthetic macrophage-activating lipopeptide 2 (MALP-2) from Amersham Pharmacia Biotech (Piscataway, NJ) and Lympholyte-M from Cedarlane (Ontario, Canada). Enzyme-linked immunosorbent assay (ELISA) kits for mouse (m)IFN-γ were obtained from Amersham Biosciences.

The following antibodies were used: antimouse NKG2D polyclonal Ab and antipan-Rae-1 polyclonal Ab (rabbit serum)

[4]To whom correspondence should be addressed.
E-mail: seya-tu@pop.med.hokudai.ac.jp
[5]Present address: Research and Education Center for Genetic Information, Nara Institute for Science and Technology, Ikoma, Nara 631-0101, Japan.
[6]These authors contributed equally to this work.

doi: 10.1111/j.1349-7006.2009.01188.x

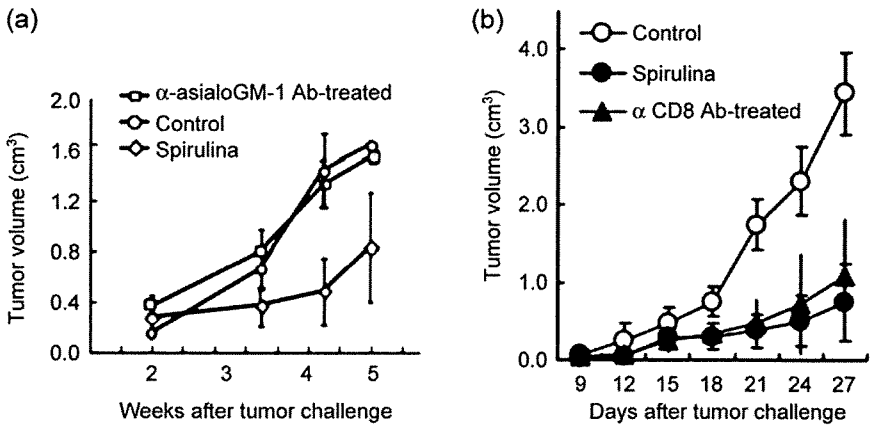

Fig. 1. AsialoGM-1 Ab-sensitive retardation of MHC-low tumor growth by oral administration of Spirulina. (a) Spirulina induces antitumor NK activation. C57BL/6 mice were separated into three groups ($n = 8$): one pretreated with anti-asialoGM-1 Ab and two with control saline, and except one control, fed with Spirulina from day 0, when B16 D8 subline was s.c. inoculated. Tumor volume was measured at intervals described in the Methods and statistical analysis was performed as described.[15] One mouse with saline only and one mouse given Spirulina and anti-asialoGM-1 Ab died of tumor after 5 weeks. We applied statistical analysis to seven live mice at the 5-week point of the two groups and declared the significance ($P < 0.05$). Represent mean ± SD. (b) CD8+ T-cells barely participate in Spirulina-mediated retardation of tumor growth. Wild-type C57BL/6 mice were grouped ($n = 5$). Spirulina extract (600 μg/600 μL) (●, ▲) or control saline (○) was orally administered to mice every other day from day −14. One group (▲) was pretreated with anti-CD8β Ab as described in the text. Then, B16D8 cells (6×10^5/head) were subcutaneously inoculated into the mice at day 0. Tumor volume was measured at indicated intervals until day 27 when the mice still survived. We declared the significance ($P < 0.05$) through statistical analysis.[15]

were established in our laboratory[16] and anti-asialoGM-1 Ab was obtained from Seikagaku Kogyo Co., Ltd. or Wako Pure Chemical Industrials, Ltd (Tokyo, Japan). Monoclonal Abs against mouse CD4 and CD8β were kindly provided by Drs T Takahashi and K Tsujimura (Aichi Cancer Center, Nagoya, Japan) as previously described.[17] Fluorescein isothiocyanate (FITC)-conjugated goat antirabbit and rat IgG $F(ab')_2$ were obtained from American Qualex (San Clemente, CA), rat IgG1κ control FITC from BD PharMingen (San Diego, CA), and hamster IgG isotype control FITC from eBioscience (San Diego, CA).

Preparation of BCG–CWS and hot-water extract of Spirulina. Spray-dried powder of *Spirulina platensis* propagated under basic conditions (pH 11) in outdoor open tanks was extracted with water in an autoclave for 1 h at 120°C. In some experiments, citric acid was added to the hot water extract to adjust the pH to 4.0.[18] The water-soluble extract was prepared by removal of insoluble fractions by centrifugation. The Spirulina extract was added to the mouse food at 1 mg/g (Clea Japan, Tokyo). In other experiments to administer accurate amounts of the extract to mice, the soluble extract of Spirulina was condensed to 1 mg/mL for oral administration as described previously.[18] In *in vitro* experiments, Spirulina extract was treated with polymyxin B (final concentration, 5 μg/mL) for 1 h at 37°C before cell stimulation to exclude the effect of possible contaminating LPS.

BCG–CWS was prepared in Dr I Azuma's laboratory (Research Institute for Immunology, Hokkaido University) as described previously.[19] The lot used in this study (Lot 10-2) consisted of mycolic acid, arabinogalactan and peptidoglycan with greater than 97% purity, and LPS contamination less than the detection limit (data not shown). Since BCG–CWS is insoluble in water and organic solvents, the oil-in-water emulsion form of BCG–PGN micelles (BCG-emulsion) was used throughout the *in vivo* study. B16 cell debris conjugated to BCG–CWS (BCG–CWS/Ag) was prepared as described below and detailed elsewhere.[15]

Mouse and cell lines. TLR2 −/−, TLR4 −/− and MyD88 −/− mice were gifts from Dr S Akira (Osaka University, Osaka) as previously reported.[15] TICAM-1 (TRIF) −/− mice were established in our laboratory.[17] Female C57BL/6 mice were purchased from Clea Japan. Mice were maintained in our institute under specific pathogen-free conditions. All animal work was performed under guidelines established by the Osaka Medical Center Institutional Animal Care and Use Committee. Mice (12-week-old female C57BL/6) were housed four per cage and allowed food and water *ad libitum*. Animal studies were carefully performed without ethical problems. In some experiments, mice were fed for 3 weeks with pathogen-free food containing 1 mg/g Spirulina extract and control food with no Spirulina, which were prepared by Clea Japan. For more precise studies 600 μg/head of the Spirulina extract was directly administered to the mouse stomach via an injector.

The B16D8 cell line was established in our laboratory as a subline of the B16 melanoma cell line.[20] This subline was characterized by its low MHC levels with no metastatic properties when injected s.c. into syngeneic C57BL/6 mice.[16,21] These cell lines were cultured in RPMI 1640/10% FCS. Tumor challenge studies were performed as previously described.[15]

Preparation of BMDCs and spleen NK cells of mice. Mouse bone marrow-derived DCs (BMDCs) were prepared as described previously.[15] Spleen NK cells were prepared by a reported method[22] with minor modifications.[23] In brief, spleen cells were passed through a nylon wool column to remove B-cells. In some cases, anti-asialoGM-1 Ab (100 μg) was injected intravenously into mice to eliminate NK cells.[17] The nylon wool-nonadherent cells were incubated in tissue culture plates for 1 h to remove adherent cells. Nonadherent cells were subjected to the MACS system (Miltenyi Biotec, Auburn, CA) for the preparation of NK cells.[23] The population was used as NK cells within 3 days.

Immunization. On days −28, −21, −14, −1 and +7 relative to the day of B16D8 challenge (Fig. 1), 5×10^6 B16D8 cells (in 90 μL) were in freeze–thaw cycles three times in PBS to prepare 'debris' and the debris was mixed with 10 μL of 1 mg/mL BCG–CWS in emulsion buffer (BCG–CWS/Ag).[15] Wild-type mice (>12 weeks old) were s.c. immunized with 30 μL of this mixture per head at the base of the tail. The administration protocol is shown in a previous report.[15] As controls, either tumor debris (Ag) only or emulsion only was used. Since BCG–CWS alone in emulsion buffer possesses immune potentiation activity upon subcutaneous (s.c) administration,[15,18] it could not be used as control for BCG–CWS/Ag.

Tumor challenge. B16D8 cells (2×10^6 cells in Fig. 1) were s.c. inoculated in the hind flank of wild-type mice. One group of

the mice was i.v. injected with anti-asialoGM-1 Ab (100 μg/100 μL) every week and the other was with mouse IgG. The tumor-challenged mice were fed with Spirulina-containing food from day 0 to the end of the study. In the next experiments, B16D8 cells (5×10^5 cells) were s.c. inoculated into mice, either preimmunized or non-immunized with BCG CWS/Ag. Mice were grouped into four, each consisting of 20 mice: group 1 with BCG–CWS/Ag and Spirulina, group 2 with BCG–CWS/Ag only, group 3 with Spirulina only and group 4 with no adjuvant. Likewise, mice were i.v. injected with anti-asialoGM-1 or anti-CD8β Abs (100 μg/100 μL) every week,[17] challenged with B16D8 and fed with Spirulina (600 μg/600 μL) every other day. The tumor sizes were compared with those of control mice. Tumor volumes were measured at regular intervals using a caliper. Tumor volume was calculated using the formula: Tumor volume (cm^3) = (long diameter) × (short diameter) × (short diameter) × 0.4.

Statistical analysis. A Student's *t*-test was used to examine the significance of the data when applicable in animal studies. Comparisons with more than two groups were done using ANOVA with appropriate *post hoc* testing. Differences were considered to be statistically significant when $P < 0.05$.

ELISA, flow cytometric (FACS) analysis of cell surface antigens. The levels of IFN-γ were determined by sandwich ELISA (Amersham Pharmacia Biotech, Buckinghamshire, UK) or the message levels assessed by quantitative PCR.[23] The practical methods for FACS were described previously.[24]

Quantitative RT-PCR. BMDCs were harvested 4 h after treatment with Spirulina extracts (50 μg/mL). The total RNA was extracted by RNeasy mini kit (Qiagen, Bothell, WA). Total RNA (0.5 μg) was incubated at 70°C for 5 min and then kept on ice for 2 min, and RT was performed as described previously.[25] The following primers were used for quantitative PCR: IFN-β forward, 5′-CCAGCTCCAAGAAAGGACGA-3′, and reverse 5′-CGCCCTGT AGGTGAGGTTGA-3′; IP-10 forward 5′-GTGTTGAGATCATT GCCACGA-3′, and reverse 5′-GCGTGGCTTCACTCCAGTTAA-3′. β-Actin was used as an internal control to normalize reactions.

Assessment of in vitro cytolytic activity. The cytolytic activity of spleen NK cells was determined by ^{51}Cr assay as described previously.[23] Effector lymphocytes were prepared from the spleen of intact C57BL/6 mice. A B16 subline (D8) or YAC-1 was used as a target cell. Target cells (0.4×10^4 cells/well) were co-incubated with the effector splenocytes at the indicated lymphocyte to target (E/T) cell ratio (typically 1, 5 and 20) in V-bottomed 96-well plates in a total volume of 200 μL of 0.5% BSA/RPMI-1640 medium at 37°C. Four hours later, the liberated ^{51}Cr in the medium was measured using a scintillation counter. Specific cytolytic activity was obtained by the formula: Specific cytotoxic activity (%) = [(experimental ^{51}Cr activity – spontaneous ^{51}Cr activity)/(total ^{51}Cr activity – spontaneous ^{51}Cr activity)] × 100. Each experiment was done in triplicate to confirm reproducibility of the results, and representative results are shown. A Student's *t*-test was used to examine the significance of the data.

Results

Tumor regression in mice given Spirulina. Retardation of tumor growth was observed in implant B16D8 tumor in mice when given Spirulina. The suppression of tumor growth by Spirulina was abrogated if the mice were treated with anti-asialoGM-1 Ab to eliminate NK cells[17] (Fig. 1a). The effect of Spirulina on tumor regression was somewhat variable in a mouse-to-mouse fashion, but was significant ($n = 8$). The mouse group with Spirulina all survived 6 weeks after tumor challenge although some died in the control and NK-depleted groups by 6 weeks. The results were confirmed with additional experiments, where NK activation occurred in mice in response to being fed Spirulina and disrupted by administration of anti-asialoGM-1 Ab (data not shown). We further confirmed that depletion of CD8+ T-cells had virtually no effect on Spirulina-mediated antitumor activity (Fig. 1b). NK activation may have occurred in mice given Spirulina to retard tumor growth.

NK activation in mice given Spirulina. We confirmed that the hot-water extract of Spirulina induces NK activation by direct NK assay. Mice (wild-type) were orally administered with the extract of Spirulina or just saline (control) every other day for 2 weeks. The NK fraction of the spleen cells was prepared by MACS beads and cultured *in vitro* in medium only (Fig. 2a). NK-mediated cytotoxicity was determined using an NK-target, YAC-1. NK activation was enhanced in the group with Spirulina compared to those without Spirulina (Fig. 2a). Similar results were obtained with the B16D8 cells as targets (data not shown). We next tested what molecular mechanisms participate in the Spirulina-mediated NK-enhanced activation. We used MyD88 –/– and TICAM-1 –/– mice to test the Spirulina NK-enhancing effect (Fig. 2b). In MyD88 –/–mice NK activation was not enhanced by administration of Spirulina, while in TICAM-1 –/– mice NK activation was enhanced by Spirulina as in wild-type mice. Hence, the TLR pathway involving MyD88, but not TICAM-1, participates in NK activation. NK cytotoxicity was already high in control mice given no Spirulina, irrespective of disruption of the TLR pathways (Fig. 2b), suggesting that other factors than TLRs also participate in *in vivo* NK activation. We found that BMDCs prepared *in vitro* elicit NK-enhancing activity in response to the extract of Spirulina (Fig. 2c,d). The ability of Spirulina to drive NK activation in BMDCs was not abrogated with TICAM-1 –/– BMDCs but abrogated with MyD88 –/– BMDCs (Fig. 2d). Consistent with the result that MyD88 rather than TICAM-1 is crucial for Spirulina-mediated NK activation by BMDC, TICAM-1-dependent mediators IFN-β and IP-10 were barely induced in Spirulina-stimulated BMDCs (Fig. 2e). Our interpretation of these results is that part of the *in vivo* NK-enhancing activity by Spirulina is attributable to the MyD88 pathway in BMDCs resulting in BMDC–NK reciprocal activation. Using this *in vitro* system, we tested if TLR2 and TLR4 are involved in the Spirulina NK-enhancing activity. TLR2/4-double deficient mice severely abrogated the response to Spirulina to reduce the Spirulina-mediated NK enhancing activity (Fig. 2c), although either one of TLR2 or 4 deficiency exhibited only a marginal effect on NK-enhancing activity by Spirulina. Thus, TLR2/4 and MyD88 participate in Spirulina-mediated BMDC-NK activation.

Additive tumor regression by BCG–CWS and Spirulina. BCG–CWS is an agonist of TLR2/4 to activate the MyD88 pathway, but does not activate NK cells,[12,13] in contrast to the Spirulina extract. MyD88 may have two arms to drive CTL and NK cells in this context. BCG–CWS/Ag subcutaneously administered effectively matures antigen-presenting dendritic cells to induce tumoricidal CTL depending upon antigens selected.[15] We next checked whether BCG–CWS/Ag and Spirulina elicit a synergistic effect on tumor regression in B16D8 melanoma-bearing mice (Fig. 3a). In this experiment, tumor burden was controlled for mice to survive greater than 6 weeks after tumor challenge. Four mouse groups ($n = 20$ each) were made to test if the tumor suppression activity depended on the host response to BCG–CWS/Ag and/or Spirulina in the same B16 implant system. Although either BCG–CWS/Ag or Spirulina alone exerted ability to regress the implant tumor, the combination of both most effectively reduced tumor sizes ($P < 0.05$) (Fig. 3a). Thus, Spirulina and BCG–CWS/Ag additively suppress tumor progression. Survival rate of mice challenged with B16D8 is also shown in Fig. 3(b). The group treated with BCG–CWS and Spirulina survived the longest, since 45% of mice in this group were alive after 9 weeks, by the time more than 80% of control mice died. Mice treated with anti-asialoGM-1 Ab all died by 9 weeks (Fig. 3b), suggesting the importance of NK cells for antitumor immune response and long survival.

doi: 10.1111/j.1349-7006.2009.01188.x

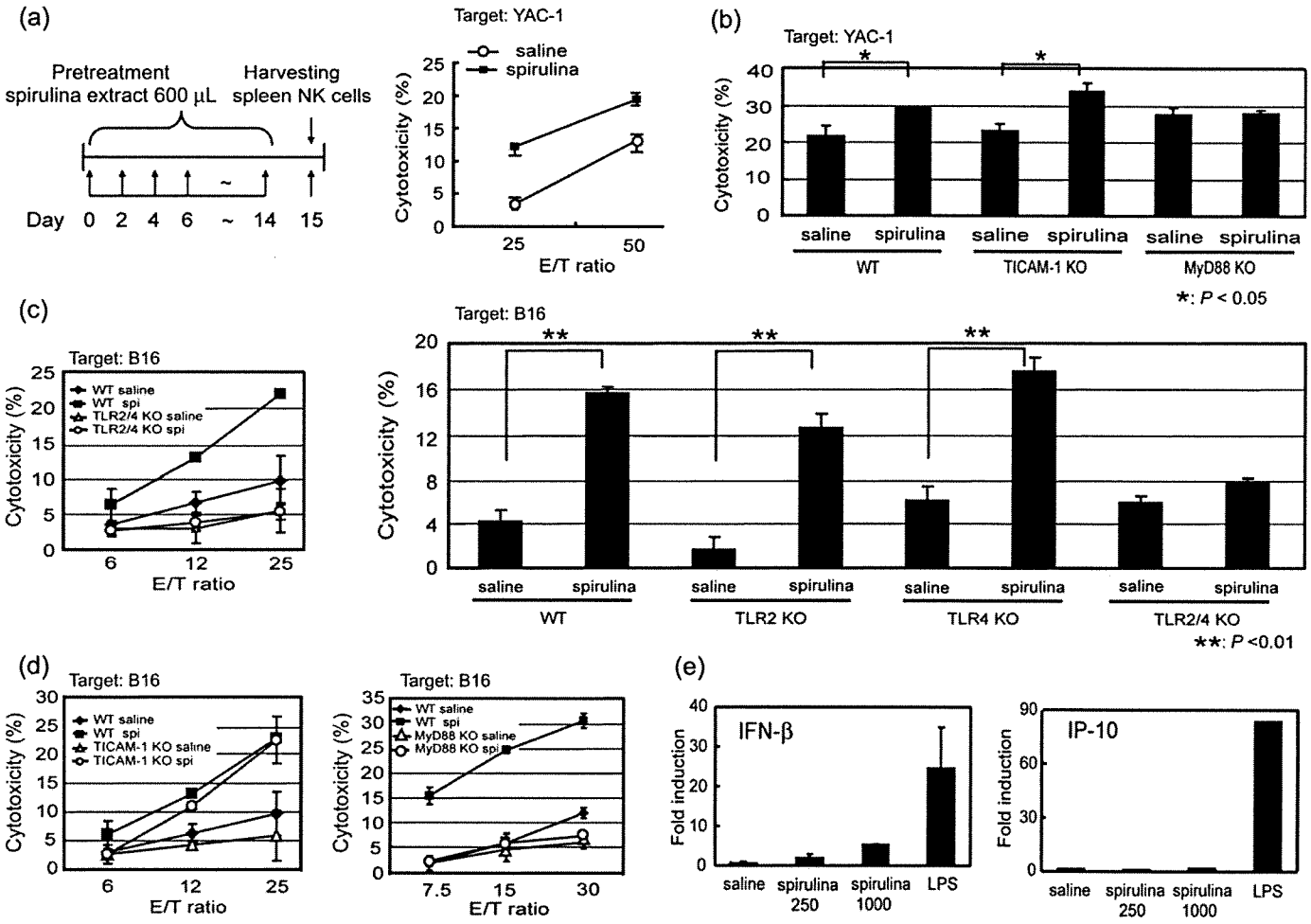

Fig. 2. Orally administered Spirulina enhances NK activation in mice. (a) YAC-1 killing activity of spleen NK cells harvested from mice with or without Spirulina. Spirulina extract (600 μg/600 μL) was orally administered into mice every other day. Two weeks later, spleen cells were harvested to isolate NK cells by MACS beads from wild-type mice. NK activity against YAC-1 or B16D8 cells (not shown) were determined at the indicated E/T ratio. (b) Participation of MyD88 in enhanced NK activation by Spirulina. NK cells were prepared from wild-type, TICAM-1 –/– or MyD88 –/– mice which had been treated with saline or Spirulina extract as in (a). NK cytotoxic activity was determined using YAC-1. (c) Spirulina effect on BMDC-NK activation was abrogated with TLR2/4 –/– BMDCs. BMDCs from wild-type and TLR2/4-double deficient mice were stimulated with Spirulina extract for 4 h and mixed with NK cells for 24 h. The mixture was incubated with ^{51}Cr-labeled target B16 cells for 4 h at the E/T ratio indicated (left panel). In the right panel, BMDCs of the indicated KO mice were admixed with NK cells as in the left panel. NK activity was determined using ^{51}Cr-labeled B16 target at a fixed E/T ratio (1:25). Percentage cytotoxicity was determined as in (a). Only slight abrogation of the Spirulina-mediated NK activation was observed in either TLR2 –/– or TLR4 –/– BMDCs under the same conditions (data not shown). (d) Spirulina acts on BMDC and augments MyD88-mediated NK reciprocal activation by BMDC. BMDCs with TICAM-1 –/– (left panel) and MyD88 –/– (right panel) were stimulated with Spirulina extract for 4 h and mixed with NK cells for 24 h. The mixture was incubated with ^{51}Cr-labeled target B16 cells for 4 h at the E/T ratio indicated. Percentage cytotoxicity was determined as (a). (e) The mRNA levels of IFN-β and IP-10 in BMDCs were determined by quantitative PCR 4 h after Spirulina stimulation. These experiments were performed three times and similar results were obtained. Representative analyses are shown.

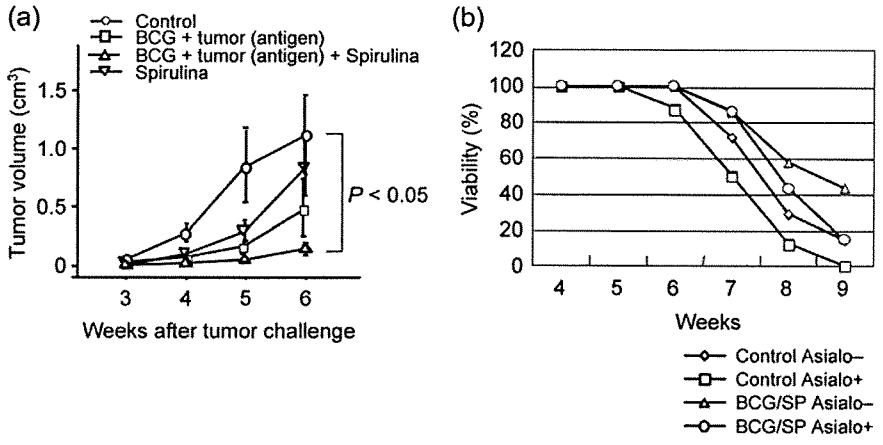

Fig. 3. Implant tumor retardation by BCG–CWS and Spirulina in mice. (a) C57BL/6 mice were separated into four groups (n = 20): group 1 with saline only, group 2 with BCG–CWS/B16 Ag, group 3 with Spirulina and group 4 with BCG–CWS/Ag and Spirulina. BCG–CWS/Ag was administered four times from day –21 to day 0,[15] while Spirulina was fed from day –21 to the end of the survey (see inset). B16D8 subline was s.c. inoculated at day 0. Tumor volume was measured at intervals and statistical analysis was performed as described.[15] (b) Mice were grouped into four (n = 20) as indicated in (a), and the effect of asialoGM-1 Ab on the survival of tumor-implant mice was analyzed. The survival rate was plotted for each group of mice.

Levels of IFN-γ in Spirulina/BCG–CWS-treated mice. IFN-γ is an effector that may be associated with prognosis of patients with BCG–CWS adjuvant immunotherapy.[26] IFN-γ was secreted in the blood of mice with tumor burden if they were treated with BCG–CWS and Ag (Fig. 4). Either BCG–CWS/Ag or Spirulina alone slightly induced IFN-γ. The levels of IFN-γ induced by Spirulina appeared low in mice compared to human volunteers.[11] Tumor antigen had no effect on the level of Spirulina-mediated IFN induction (data not shown). Notably, significantly high levels of IFN-γ were detected in mice treated with both BCG–CWS/Ag and Spirulina (Fig. 4). Skin reaction reflecting BCG hypersensitivity was observed in the relevant group (data not shown). No or less skin reaction was observed in the group with BCG–CWS/Ag and Spirulina. Spirulina alone did not induce skin reaction.

Rae-1-positive B16 cells were eliminated by Spirulina. B16D8 cells in implant tumor of C57BL/6 mice consisted of Rae-1-positive and -negative cells. The cells were inoculated into the mice which were fed and/or treated with the material indicated (Fig. 5). Implanted B16 tumor cells were extracted from the tumor-bearing mice 5 weeks after tumor challenge, stained with the indicated Abs and analyzed by FACS (Fig. 5), where mean fluorescence intensities are shown in the insets. In the group given no Spirulina, tumor cells consisted of Rae-1-positive and -negative populations, whereas in the group given Spirulina, the Rae-1-positive population was selectively diminished. The group treated with Spirulina and anti-asialoGM-1 Ab possessed the Rae-1-positive population. Other markers including MHC class I and class II were neither detectable nor different among the groups. Although other NK-activation ligands were detected in message levels, they still remained in the Rae-1-negative cells (data not shown). Thus, Rae-1-positive tumor cells are selectively eliminated by Spirulina-derived NK cells in this mouse system.

This issue was confirmed using an *in vitro* assay. NK cells reciprocally activated by Spirulina-treated BMDCs damaged B16D8 cells (Fig. 6a). The NK-mediated B16D8 killing was largely blocked by the addition of anti-NKG2D Ab (Fig. 6a).

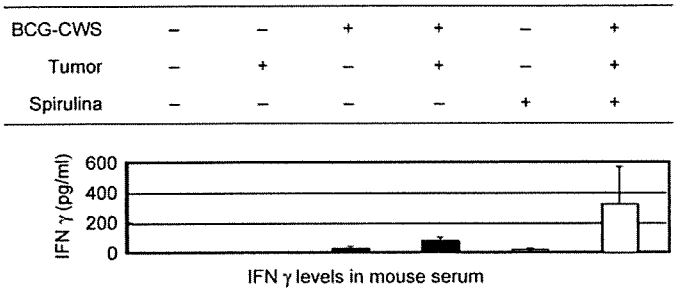

Fig. 4. Serum level of IFN-γ in tumor-bearing mice given BCG–CWS and/or Spirulina. Mice were treated with BCG–CWS/B16 Ag and/or Spirulina and inoculated with B16 tumor at day 0 as in Fig. 3. Forty-eight hours after tumor implantation, mouse sera were obtained from their tails and the levels of IFN-γ were determined by ELISA.

Without BMDCs, Spirulina extract treatment barely activated NK cells (data not shown). Thus, NK-mediated B16D8 killing was attributable to interaction between tumor cell Rae-1 and NK cell NKG2D, which is supported by Spirulina-dependent maturation of BMDC, as there is no direct route for Spirulina-mediated NK activation.

Spirulina-mediated B16D8 growth was largely abrogated in MyD88 –/– mice (Fig. 6b). Antitumor NK activation predicted in this study may occur in tumor-bearing mice through being given Spirulina.

Discussion

We demonstrated that tumor growth is retarded in mice given Spirulina. Unique points in this study are: (i) Rae-1-positive tumor cells are selectively eliminated in Spirulina-fed mice; and (ii) marked tumor regression is observed in mice with combinational administration of BCG–CWS/Ag and Spirulina. Synergistic effects on tumor regression and increase of serum

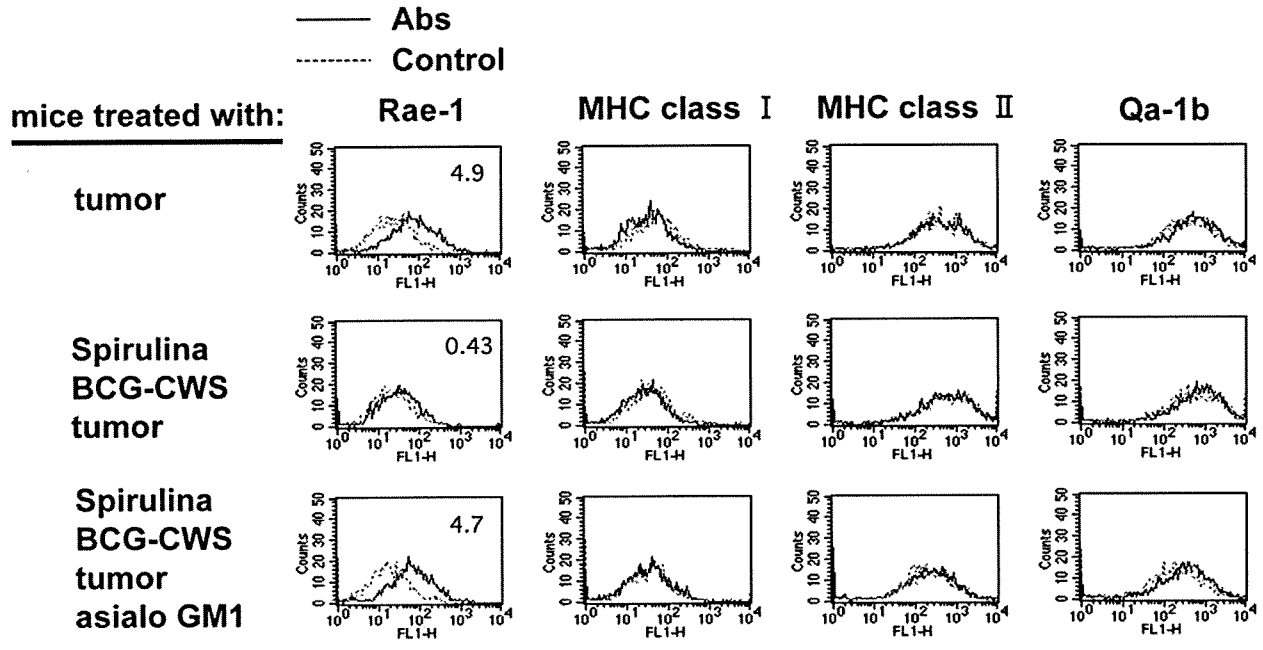

Fig. 5. Rae-1 and MHC levels in the implant tumor of mice. Mice were treated with anti-asialoGM-1 Ab, Spirulina, B16 tumor Ag and/or BCG–CWS as in Fig. 3, and inoculated with B16 cells; prescriptions are indicated in the left column. Five weeks later, the cells were harvested and dispersed in PBS–EDTA. The levels of Rae-1, MHC class I, MHC class II and Qa-1b were assessed by FACS using their specific Abs.[16] Specific mean fluorescence intensities of Rae-1 are indicated in the fluorograms as described elsewhere.[16]

doi: 10.1111/j.1349-7006.2009.01188.x

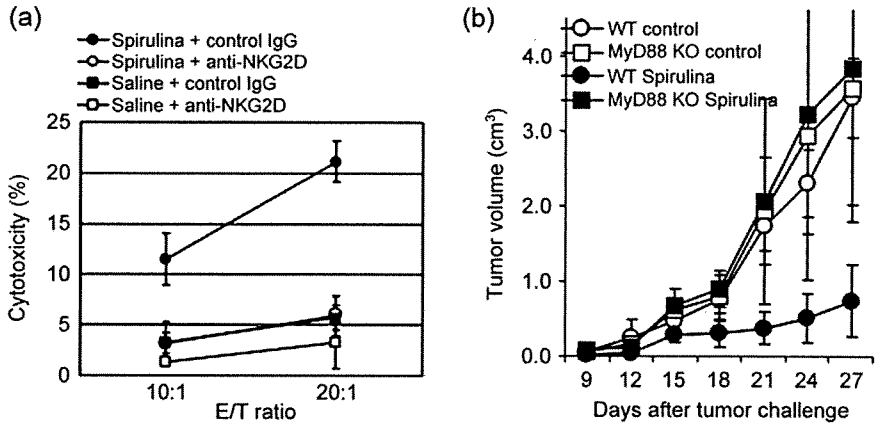

Fig. 6. Spirulina NK cells damage B16D8 tumor cells through MyD88 and NKG2D receptor. (a) NK cells kill B16D8 cells through NKG2D after incubation with Spirulina-treated BMDCs. BMDCs from wild-type mice were stimulated with Spirulina extract for 4 h and mixed with NK cells for 24 h (DC:NK = 1:3). The mixture was incubated with anti-NKG2D Ab or control IgG and ^{51}Cr-labeled target B16 cells for 4 h at the E/T ratio indicated. (b) MyD88 is crucial for Spirulina-mediated tumor growth retardation. Wild-type and MyD88 –/– mice were grouped as shown. Spirulina extract (600 μg/600 μL) (●, ■) or control saline (○, □) was orally administered to wild-type and MyD88 –/– mice (n = 5) every other day from day –14. B16D8 cells (6 × 10^5/head) were subcutaneously inoculated into the mice at day 0. Tumor volume was measured at indicated timed intervals until day 27 when the mice survived, and statistical analysis was performed as in Fig. 1 ($P < 0.05$).

IFN-γ level were observed in mice by combination treatment with BCG–CWS/Ag and Spirulina. BCG–CWS/Ag induces CTL via TLR2/4 in myeloid DCs in a MyD88-dependent manner.[15] In this study, Spirulina activates NK cells also via TLR2/4 in BMDCs in a MyD88-dependent manner. These reports suggest that simultaneous attack by CTL and NK more effectively regresses tumor cells in mouse tumor implant models.

Our *in vitro* findings on Spirulina allowed us to interpret that the Spirulina extract activates the MyD88 pathway in BMDCs to evoke activation of mouse NK cells (Fig. 2). What mechanisms activate the MyD88 pathway to drive NK cells in Spirulina-stimulated BMDCs is an intriguing issue, since other TLR2/4 ligands mainly engage CTL induction, but not NK activation, via the MyD88 pathway in BMDCs.[27,28] Difference in downstream signal events may cause the different outcomes of NK/CTL induction in BMDCs. Studying the Spirulina-activated MyD88 pathway will be an important issue to clarify how it is possible to have two TLR2/4 agonists activate NK and CTL.

There appear several routes for activation of NK cells. The BMDC-mediated NK activation serves an important route for NK-mediated tumor clearance.[29–31] We demonstrated that the TICAM-1 (TRIF) pathway in BMDCs participates in the DC–NK reciprocal activation.[17,27,32] In contrast, most of the non-DNA/RNA adjuvants currently available originate from bacteria and activate the MyD88 pathway of TLR2 and/or TLR4 in DCs, but they barely induce NK activation.[17,28] In this context, BCG–CWS expressed high tumor-killing activity (Fig. 3a), but this activity was barely abrogated by administration of anti-asialoGM-1 Ab (data not shown). Further, Spirulina appears to differ from LPS in its adjuvant activity, since LPS simultaneously activates the MyD88 and TICAM-1 pathways to evoke the systemic cytokine storm. The Spirulina extract is unique because it has an ability to activate NK cells without inducing type I IFNs.

Spirulina-mediated IFN-γ production is greatly enhanced in mice by simultaneous administration of BCG–CWS/Ag, similar to humans.[33] How Spirulina participates in IFN-γ production is a future question. Spirulina ultimately activates T- and NK cells in mice, although IFN-γ is poorly induced in mice compared to human volunteers with only Spirulina.[11] Direct addition of Spirulina to splenic lymphocytes neither results in NKG2D up-regulation nor induces enhanced B16D8 cell killing (data not shown), suggesting that cell populations other than DCs in the spleen barely participate in this event. There is a report that the MAPK pathway of BMDCs participates in promotion of NK activation by BMDCs.[34] If this is the case, the NK-enhancing effect by Spirulina in human patients can be evaluated in the mouse model and IFN-γ production is a good marker for NK activation.

Previous studies on patients with cancer suggested that Spirulina constituents serve as protective agents against oral cancers[35] in terms of tumor progression and metastasis,[36] although the results are from non-randomized trials. These reports were reminiscent of the antitumor functions of Spirulina, some of which would be derived from β-carotene, an effective antioxidant.[37] Indeed, the serum levels of β-carotene are consistently low in patients with cancer.[37,38] Our present study may offer additional evidence that NK activation is a representative of the Spirulina-mediated antitumor immunity.

However, a point remains unsettled that the constituents of Spirulina taken up via the intestine and colon do not always correspond to those of the extract of Spirulina. *In vitro* studies where Spirulina was added to NK cells or BMDCs appear not to be simply comparable with the *in vivo* studies using mice. In other reports, Spirulina orally taken significantly reduced IL-4 levels in individuals with allergic rhinitis by a randomized double-blinded trial.[39] Another report suggested that Spirulina enhances IgG1 and IgA production but not IgE production by modulating the mucosal immune system.[9] Spirulina may skew the Th2 polarization to a Th1-like state in allergic patients. We should identify the Spirulina constituents associated with activation of mucosal immunity and absorbed into the circulation.

Since cancers are usually established by circumventing the host immune system including NK and CTL, tumor cells generally possess poor immunogenicity by expressing low levels of MHC class I and ligands for NK-activating receptors including NKG2D.[40] It is notable that these receptor levels are regulated by IFN-γ. It has been reported that during BCG adjuvant therapy the increased serum level of IFN-γ 18 h after s.c. injection of BCG–CWS is a marker for evoking the innate immune response.[26] In mouse experimental models using syngeneic transplantable tumors, MHC class I-expressing tumor cells were selectively eliminated by BCG–CWS/Ag s.c. injection,[15] and the serum levels of IFN-γ were increased in the case of Spirulina, too. Nevertheless, tumor cells with low MHC expression remain,

resulting in MHC-negative tumor progression. This study clearly shows that tumor growth is suppressed in an MHC-negative/Rae-1-positive population of tumor cells by treatment of tumor-implant mice with Spirulina, which can induce NK activation to damage tumor cells via NKG2D receptors.

In human cancer patients receiving BCG–CWS therapy, tumor cells have not completely disappeared from the primary region,[41] although patients' quality of life (QOL) scores are increased in response to the BCG–CWS therapy. Similar observations were reported in patients with bladder cancer who selected BCG immunotherapy.[42] Growing the low-MHC tumor cells may account for the incomplete remission of tumors in patients with cancer.

We offer the possible immune therapy in combination with BCG–CWS and Spirulina in this communication. Additive tumor cytotoxicity based on BCG–CWS/Ag and Spirulina suggests that they elicit different effectors, putative CTL and NK. Their combinational function merely targets the MyD88 pathway and is clearly distinct from that of LPS that induces toxic shock. Although which constituents of the Spirulina extract are responsible for NK enhancement, and why Spirulina and BCG–CWS differentially activate the TLR2/4-mediated MyD88 pathway in DCs should be further investigated, this is the fist report predicting that the combination of BCG–CWS/Ag and Spirulina is applicable to immunotherapy for patients with tumor mass of variable MHC levels. We favor the premise that Spirulina is a candidate for NK activator applicable to cancer patients by oral usage.

Acknowledgments

This work was supported in part by CREST, Japan Science and Technology Corporation, by Grants-in-Aid from the Ministry of Education, Science, and Culture (Specified Project for Advanced Research) and the Ministry of Health, Labor, and Welfare of Japan, by the Akiyama Foundation and Yakulto Foundation. Financial support by the Sapporo Biocluster 'Bio-S' Knowledge Cluster Initiative of the MEXT, and the Program of Founding Research Centers for Emerging and Re-emerging Infectious Diseases, MEXT are gratefully acknowledged. We are grateful to Drs K Funami, M Shingai, M Sasai, A Matsuo, H Shime and H Oshiumi for their critical discussions and Ms Hatsugai and Ms Sato for technical support. Thanks also to Drs S Akira (Osaka University, Osaka) and T Takahashi (Aichi Cancer Center, Nagoya) for providing knockout mice and specific Abs, respectively.

References

1 Medzhitov R, Janeway CA Jr. Innate immunity: the virtues of a nonclonal system of recognition. *Cell* 1997; **91**: 295–8.
2 Takeda Y, Kaisho T, Akira S. Toll-like receptors. *Annu Rev Immunol* 2003; **21**: 335–76.
3 Furrie E, Macfarlane S, Thomson G, Macfarlane GT, George T. Toll-like receptors-2, -3 and -4 expression patterns on human colon and their regulation by mucosal-associated bacteria. *Immunology* 2005; **115**: 565–74.
4 Dostert C, Meylan E, Tschopp J. Intracellular pattern-recognition receptors. *Adv Drug Deliv Rev* 2008; **60**: 830–40.
5 Belay A. Spirulina (Arthrospira): production and quality assurance. In: Gershwin ME, Belay A, eds. *Spirulina in human nutrition and health*. New York: CRC Press, 2007; 1–25.
6 Tornabene TG, Bourne TF, Raziuddin S, Ben-Amotz A. Lipid and lipopolysaccharide constituents of cyanobacterium *Spirulina platensis* (Cyanophyceae, Nostocales). *Mar Ecol* 1985; **22**: 121–5.
7 Dillon JC, Phuc AC, Dubacq JP. Nutritional value of the alga Spirulina. *World Rev Nutr Diet* 1995; **77**: 32–46.
8 Hayashi T, Hayashi K, Maeda M, Kojima I. Calcium spirulan, an inhibitor of enveloped virus replication, from a blue-green alga *Spirulina platensis*. *J Nat Prod* 1996; **59**: 83–7.
9 Hayashi O, Katoh T, Okuwaki Y. Enhancement of antibody production in mice by dietary *Spirulina platensis*. *J Nutr Sci Vitaminol (Tokyo)* 1994; **40**: 431–41.
10 Mao TK, Van de Water J, Gershwin ME. Effects of a Spirulina-based dietary supplement on cytokine production from allergic rhinitis patients. *J Med Food* 2005; **8**: 27–30.
11 Hirahashi T, Matsumoto M, Hazeki K, Saeki Y, Ui M, Seya T. Activation of the human innate immune system by spirulina: augmentation of interferon gamma production and NK cytotoxicity by oral administration of spirulina. *Int Immunopharmac* 2002; **2**: 423–34.
12 Seya T, Akazawa T, Matsumoto M, Begum NA, Azuma I, Toyoshima K. Innate immune therapy for cancer: application of BCG-CWS and spirulina to patients with lung cancer. *Anticancer Res* 2003; **23**: 4369–76.
13 Tsuji S, Matsumoto M, Takeuchi O *et al.* Maturation of human dendritic cells by cell-wall skeleton of Mycobacterium bovis Bacillus Calmette-Guerin: involvement of Toll-like receptors. *Infect Immun* 2000; **68**: 6883–90.
14 Uehori J, Tsuji S, Matsumoto M *et al.* Simultaneous blocking of human Toll-like receptor 2 and 4 suppresses myeloid dendritic cell maturation induced by Mycobacterium bovis bacillus Calmette-Guérin (BCG) -peptidoglycan (PGN). *Infect Immun* 2003; **71**: 4238–49.
15 Akazawa T, Masuda H, Saeki Y *et al.* Adjuvant-mediated tumor regression and tumor-specific CTL induction are impaired in MyD88-deficient mice. *Cancer Res* 2004; **64**: 757–64.
16 Masuda H, Saeki Y, Nomura M *et al.* High levels of RAE-1 isoforms on mouse tumor cell lines assessed by anti-'pan' RAE-1 antibody confer tumor susceptibility to NK cells. *Biochem Biophys Res Commun* 2002; **290**: 140–5.
17 Akazawa T, Okuno M, Okuda Y *et al.* Antitumor NK activation induced by the Toll-like receptor3-TICAM-1 (TRIF) pathway in myeloid dendritic cells. *Proc Natl Acad Sci USA* 2007; **104**: 252–7.
18 Quoc KP, Dubacq JP. Effect of growth temperature on the biosynthesis of eukaryotic lipid molecular species by the cyanobacterium *Spirulina platensis*. *Biochim Biophys Acta* 1997; **1346**: 237–46.
19 Azuma I, Ribi EE, Meyer TJ, Zbar B. Biologically active components from mycobacterial cell walls. I. Isolation and composition of cell wall skeleton and component P3. *J Natl Cancer Inst* 1974; **52**: 95–101.
20 Tanaka H, Mori Y, Ishii H, Akedo H. Enhancement of metastatic capacity of fibroblast–tumor cell interaction in mice. *Cancer Res* 1988; **48**: 1456–9.
21 Saeki Y, Seya T, Hazeki O, Hazeki K, Ui M, Akedo H. Phosphatidylinositol 3 kinase inhibitors block matrix adhesion and experimental metastasis of high metastatic mouse hepatoma clones. *J Biochem (Tokyo)* 1998; **124**: 1020–5.
22 Uenaka A, Ono T, Akisawa T, Wada H, Yasuda T, Nakayama E. Identification of a unique antigen peptide pRL1 on BALB/c RL male 1 leukemia recognized by cytotoxic T lymphocytes and its relation to the Akt oncogene. *J Exp Med* 1994; **180**: 1599–607.
23 Ebihara T, Masuda H, Akazawa T *et al.* NKG2D ligands are induced on human dendritic cells by TLR ligand stimulation and RNA virus infection. *Int Immunol* 2007; **19**: 1145–55.
24 Nishiguchi M, Matsumoto M, Takao T *et al.* Mycoplasma fermentans lipoprotein M161Ag-induced cell activation is mediated by Toll-like receptor 2: role of N-terminal hydrophobic portion in its multiple functions. *J Immunol* 2001; **166**: 2610–6.
25 Livak KJ, Schmittgen TD. Analysis of relative gene expression data using real-time quantitative PCR and the 2 (-Delta Delta C (T) method. *Methods* 2001; **25**: 402–8.
26 Hayashi A, Noda A. Does the cell wall skeleton from Bacille Calmette-Guerin directly induce interferon-gamma, independent of interleukin-12? *Jpn J Clin Oncol* 1996; **26**: 124–7.
27 Seya T, Matsumoto M. The extrinsic RNA-sensing pathway for adjuvant immunotherapy of cancer. *Cancer Immunol Immunother* 2009, January 31 [Epub ahead of print].
28 Seya T, Hazeki K, Inoue N, Matsumoto M. Pattern-recognition confers driving various cellular effectors on dendritic cells. *Cancer Sci* 2009; in press.
29 Hayakawa Y, Smyth MJ. NKG2D and cytotoxic effector function in tumor immune surveillance. *Semin Immunol* 2006; **18**: 176–85.
30 Moretta L, Ferlazzo G, Bottino C *et al.* Effector and regulatory events during natural killer–dendritic cell interactions. *Immunol Rev* 2006; **214**: 219–28.
31 Gerosa F, Baldani-Guerra B, Nisii C, Marchesini V, Carra G, Trinchieri G. Reciprocal activating interaction between natural killer cells and dendritic cells. *J Exp Med* 2002; **195**: 327–33.
32 Matsumoto M, Seya T. TLR3 signaling inducing IFN in response to dsRNA and polyI. *C Adv Drug Deliv Rev* 2008; **60**: 805–12.
33 Seya T, Ebihara T, Kodama K, Hazeki K, Matsumoto M. NK activation induced by Spirulina. In: Gershwin ME, Belay A, eds. *Spirulina in human nutrition and health*. New York: CRC Press, 2007, 195–203.
34 Pisegna S, Pirozzi G, Piccoli M, Frati L, Santoni A, Palmieri G. p38 MAPK activation controls the TLR3-mediated up-regulation of cytotoxicity and cytokine production in human NK cells. *Blood* 2004; **104**: 4157–64.
35 Mathew B, Sankaranarayanan R, Nair PP *et al.* Evaluation of chemoprevention of oral cancer with *Spirulina fusiformis*. *Nutr Cancer* 1995; **24**: 197–202.

doi: 10.1111/j.1349-7006.2009.01188.x

36 Mishima T, Murata J, Toyoshima M *et al.* Inhibition of tumor invasion and metastasis by calcium spirulan (Ca-SP), a novel sulfated polysaccharide derived from a blue-green alga, Spirulina platensis. *Clin Exp Metastasis* 1998; **16**: 541–50.
37 Ramaswamy G, Rao VR, Kumaraswamy SV, Anantha N. Serum vitamins' status in oral leucoplakias: a preliminary study. *Eur J Cancer B Oral Oncol* 1996; **32B**: 120–2.
38 Pappalardo G, Maiani G, Mobarhan S *et al.* Plasma (carotenoids, retinol, alpha-tocopherol) and tissue (carotenoids) levels after supplementation with beta-carotene in subjects with precancerous and cancerous lesions of sigmoid colon. *Eur J Clin Nutr* 1997; **51**: 661–6.
39 Mao TK, Van de Water J, Gershwin ME. Effects of Spirulina-based dietary supplement on cytokine production from allergic rhinitis patients. *J Med Food* 2005; **8**: 27–30.
40 Cerwenka A, Lanier LL. Natural killer cells, viruses and cancer. *Nat Rev Immunol* 2001; **1**: 41–9.
41 Kodama K, Higashiyama M, Takami K *et al.* Innate immune therapy with a BCG cell wall skeleton for lung cancer: a case presentation and a case control study. *Surg Today* 2009; **39**: 194–200.
42 Alexandroff AB, Jackson AM, O'Donnell MA, James K. BCG immunotherapy of bladder cancer: 20 years on. *Lancet* 1999; **353**: 1689–94.

Obstructing Shedding of the Immunostimulatory MHC Class I Chain–Related Gene B Prevents Tumor Formation

Jennifer D. Wu,[1] Catherine L. Atteridge,[1] Xuanjun Wang,[1] Tsukasa Seya,[3] and Stephen R. Plymate[1,2]

Abstract

Purpose: Clinical observations have suggested that shedding of the MHC class I chain–related molecule (MIC) may be one of the mechanisms by which tumors evade host immunosurveillance and progress. However, this hypothesis has never been proven. In this study, we tested this hypothesis using a prostate tumor model and investigated the effect of shedding of MIC on tumor development.

Experimental Design: We generated a shedding-resistant noncleavable form of MICB (MICB.A2). We overexpressed MICB.A2, the wild-type MICB, and the recombinant soluble MICB (rsMICB) in mouse prostate tumor TRAMP-C2 (TC2) cells and implanted these cells into severe combined immunodeficient mice.

Results: No tumors were developed in animals that were implanted with TC2-MICB.A2 cells, whereas all the animals that were implanted with TC2, TC2-MICB, or TC2-rsMICB cells developed tumors. When a NKG2D-specific antibody CX5 or purified rsMICB was administered to animals before tumor implantation, all animals that were implanted with TC2-MICB.A2 cells developed tumors. *In vitro* cytotoxicity assay revealed the loss of NKG2D-mediated natural killer cell function in these prechallenged animals, suggesting that persistent levels of soluble MICB in the serum can impair natural killer cell function and thus allow tumor growth.

Conclusions: These data suggest that MIC shedding may contribute significantly to tumor formation by transformed cells and that inhibition of MIC shedding to sustain the NKG2D receptor-MIC ligand recognition may have potential clinical implication in targeted cancer treatment.

Expression of murine NKG2D ligands on tumor cells has been shown to be effective in activating natural killer (NK)-mediated tumor elimination experimentally (1–4). In murine systems, identified NKG2D ligands include the retinoic acid early inducible family of proteins RAE-1 (1, 2), the minor histocompatibility antigen H60 (1, 2), and the murine ULBP-like transcript 1 (4, 5). Cells expressing these molecules are sensitive to the cytotoxicity of mouse NK cells. Ectopic expression of RAE-1 and H60 results in rejection of tumor cell lines expressing normal levels of MHC I molecule (2–4). Immunodepletion and other experiments showed that the tumor rejection is due to NK and CD8 T cells (2, 3). NKG2D neutralization *in vivo* enhances host sensitivity to carcinogen-induced spontaneous tumor initiation (6). These studies have proven the principle function of the NKG2D ligand receptor-mediated NK cell immunity in tumor rejection.

In humans, the MHC class I chain–related molecule MICA and MICB (generally termed as MIC) are the most investigated NKG2D ligands, which were proposed to play roles in tumor rejection (7–9). MIC is rarely expressed by normal human tissues but induced in most human epithelial tumors (10–13). Expression of MIC on the tumor cell surface can markedly enhance the sensitivity of tumor cells to NK cells *in vitro* and has been shown to inhibit the growth of human gliomas or small lung carcinomas in experimental models (14, 15). These studies suggested that NK cells can potentially eliminate MIC-positive tumor cells in cancer patients. However, as clinically observed, most of the human epithelial tumors are found to be MIC-positive rather than MIC-negative (10–13), which suggests the functional compromise of the MIC ligand-NKG2D receptor system in cancer patients to permit the growth of MIC-positive tumor cells. We and others have shown that tumor-derived soluble MIC as a result of tumor shedding is one of the factors causing the ineffectiveness of NKG2D-mediated immunity in cancer patients (13, 16–21). *In vitro* studies have shown that engagement of soluble MICA to NKG2D results in marked reduction in surface NKG2D expression on NK and T cells (13, 16, 21). Thus, soluble MIC is believed to induce down-modulation of NKG2D expression on systemic and tumor-infiltrated NK and T cells and thus result in functional impairment of NK and T cells in MIC-positive cancer patients (13, 16, 17). Reduction in the density of MIC expressed on the tumor cell surface due to MIC shedding from tumors is also proposed to be one of the mechanisms for tumor evasion (21).

Authors' Affiliations: [1]Department of Medicine, University of Washington; [2]Geriatric Research, Education and Clinical Center, Veterans Affairs Puget Sound Health Care System, Seattle, Washington and [3]Department of Microbiology and Immunology, Hokkaido University Graduate School of Medicine, Sapporo, Japan

Received 5/19/08; revised 8/12/08; accepted 8/20/08.

Grant support: DOD-USMRC New Investigators Grant W81XWH-04-1-0577 and IDEA Development Award W81XWH-06-1-0014, NW Prostate SPORE Program, and NIH Temin Award 1K01CA116002 (J.D.Wu).

The costs of publication of this article were defrayed in part by the payment of page charges. This article must therefore be hereby marked *advertisement* in accordance with 18 U.S.C. Section 1734 solely to indicate this fact.

Requests for reprints: Jennifer D. Wu, Department of Medicine, University of Washington, 325 9th Avenue, Box 359625, Seattle, WA 98104. Phone: 206-341-5349; Fax: 206-341-5302; E-mail: wuj@u.washington.edu.

doi:10.1158/1078-0432.CCR-08-1305

Translational Relevance

In humans, the MHC class I chain-related molecules MICA and MICB (generally termed MIC) are frequently found expressed on epithelial-originated tumor cells. MIC is a ligand for the activating NK cell receptor NKG2D. Engagement of tumor-expressed MIC to NKG2D can activate NK cell tumor-lytic activity *in vitro*. Thus, expression of MIC on tumor cells is proposed to play a significant role in tumor immunosurveillance. However, as observed in many cancer patients, majority of the tumors remain MIC positive, suggesting the ineptness of the NKG2D-mediated NK cell function. We and others have shown that shedding of MIC by tumor cells can impair NK cell function in cancer patients. These clinical studies prompted the hypothesis that tumor shedding of MIC may be one of the mechanisms by which MIC-positive tumors evade NK cell immunosurveillance and progress. This study tested this hypothesis *in vivo* using a prostate tumor model and for the first time showed that interfering with shedding of MIC could prevent tumor formation. Our study suggests that shedding of MIC may contribute significantly to tumor formation by transformed cells and thus inhibiting tumor shedding of MIC may have potential therapeutic implication in targeted cancer therapy.

These compelling clinical data suggest that MIC shedding from tumor cells is likely associated with tumor progression, which has prompted the hypothesis that tumor shedding of MIC is the mechanism by which MIC-positive tumors evade NK cell immunosurveillance and progress in cancer patients. However, it is impossible to test this hypothesis clinically. Taking the advantage that human MICB can be recognized by mouse NKG2D (22, 23) and that only the extracellular $\alpha1\alpha2$ domain of MIC interacts with NKG2D (24–26), here we test the hypothesis experimentally that shedding of MIC permits tumor growth and that sustained interaction between NKG2D and membrane-integrated form of MIC can cause tumor rejection. Using a well-characterized prostate tumor model TRAMP-C2 (TC2; ref. 27), we show for the first time that expression of the shedding-resistant but not the natural form of MICB prevents tumor formation by transformed cells.

Materials and Methods

Cells. TC2 cell line (gift of Dr. N.M. Greenberg, Fred Hutchinson Cancer Research Center) was maintained in DMEM as described (27). RMA-Rae-1β cells (gift of Dr. D. Raulet, Berkeley) was maintained in RPMI 1640 supplemented with 10% FCS. Eco-phoenix cells (Orbigen) were maintained in DMEM supplemented with 10% fetal bovine serum.

DNA construction, transfection, and transduction. cDNA encoding full-length human MICB (allele 0101; ref. 28) was kindly provided by Dr. A. Steinle (University of Tubingen) and subcloned into the retroviral vector pBMNZ-IRES-GFP (Orbigen). To generate recombinant soluble MICB (rsMICB), cDNA encoding the extracellular domain of MICB was amplified by PCR. To generate a putative shedding-resistant form of MICB (designated as MICB.A2), amino acids 215 to 274 of MICB were replaced with the comparable sequence of the α3 domain of HLA-A2 using recombinant PCR of the cDNA sequences (29). rsMICB-FLAG fusion peptide was generated by tagging the cDNA sequence of FLAG (DKYDDDK) to the 3′-end of the rsMICB cDNA using PCR. Error-free amplified cDNAs were identified by sequencing and subcloned into the retroviral vector pBMNZ-IRES-GFP (Orbigen). Plasmids were transfected into Eco-phoenix packaging cells to generate retrovirus. TC2 cells were transduced with respective retrovirus. Stable GFP-positive cell population was isolated by drug selection and sorted by flow cytometry.

Affinity purification of rsMICB and rsMICB-FLAG peptides. The HiTrip NHS-activated column (GE Healthcare) was conjugated with the monoclonal antibody (mAb) 6D4.6 (Santa Cruz Biotechnology) before loading with conditioned medium from TC2-rsMICB or TC2-rsMICB-FLAG cells. After washing, rsMICB or rsMICB-FLAG was eluted with 100 mmol/L sodium citrate (pH 2.5) and neutralized immediately with 1.5 mol/L Tris (pH 8.8).

Immunoprecipitation and Western blotting. Supernatant was collected from TC2-MICB cell culture and passed through a 0.45 μm filter to remove cell debris. Cells were washed and lysed with lysis buffer [50 mmol/L HEPES (pH 7.5), 150 mmol/L NaCl, 1.5 mmol/L $MgCl_2$, 1 mmol/L EGTA, 1% Triton X-100]. Clear supernatant and lysates were incubated with the mAb 6D4.6. Immunocomplexes were collected using protein A/G-agarose (Pierce). PNGase F (New England Biolabs) treatment was carried overnight at 37°C. Immunocomplexes were separated on a 4% to 15% SDS-PAGE, blotted onto a nitrocellulose membrane, and probed with goat anti-MICB antibody AF1599 (R&D Systems). Immunoreactive proteins were detected by incubating the blot with a horseradish peroxidase-conjugated secondary antibody (Pharmacia) and enhanced chemiluminescence reagents (Pharmacia).

MICB shedding assay and (s)MICB ELISA. Cells were seeded at the density of 4×10^5 per well in a 6-well plate in complete medium overnight and replaced with 1 mL/well serum-free medium for 6 h. Supernatant was collected and filtered through 0.45 μm filter. Cells were lysed with 1 mL lysis buffer. Amount of soluble MICB in the supernatant and MICB in the cell lysates was measured using human MICB DuoSet sandwich ELISA kit (R&D Systems). For measuring mouse serum levels of soluble MICB, serum was diluted 1:2 with PBS for ELISA assay.

In vivo *study.* Animal studies were approved by the Institutional Animal Care and Use Committee. Six to 10 severe combined immunodeficient (SCID) male mice (6-week old Harlan-Sprague-Dawley) were used in each group. The following cells (1×10^6 per mouse) were subcutaneously injected into respective group of animals: TC2, TC2-MICB, TC2-MICB.A2, and TC2-rsMICB. All animals were monitored for tumor growth for up to 12 weeks. Tumor volume was estimated using the formula: $V = L \times W^2 / 2$. Animals were euthanized when tumor volumes reached 1,000 mm^3. Tumors, spleens, and peripheral blood were terminally collected. Serum was separated by centrifugation and used for rsMICB ELISA.

In vivo *NKG2D blocking or neutralization.* To block NKG2D receptor, 100 μg of the functional grade of anti-NKG2D blocking antibody CX5 (eBiosciences) were injected intraperitoneally on the day before and the day after tumor implantation and thereafter every 3 days. Blocking was confirmed by flow cytometry of peripheral lymphocytes collected from orbital sinus bleeding with PE-conjugated CX5 (eBiosciences). To modify NKG2D function, animals were injected intraperitoneally with 50 ng purified rsMICB before implantation of TC2-MICB.A2 cells and thereafter twice a week for 4 weeks. Blood was collected once a week from sinus orbital bleeding and serum levels of rsMICB were measured by ELISA.

Flow cytometry. For detection of cell surface expression of NKG2D ligands, TC2 and its derivative cells were trypsinized, blocked with anti-mouse CD16/CD32 (eBiosciences), and incubated with anti-MICA/B mAb 6D4.6 or anti-MICB MAB1599 (R&D Systems) or anti-pan-RAE-1 mAb17582 (R&D Systems) followed by a PE-conjugated secondary

reagent. For detection of rsMICB expression, the BD Cytofix/Cytoperm kit (BD Sciences) was used. Briefly, TC2-rsMICB cells were cultured in the presence of BD GolgiPlug for 3 h to prevent the secretion of rsMICB before harvesting. Cells were resuspended in BD fixation/permeabilization solution for 20 min at 4°C and incubated with 6D4.6 followed with PE-conjugated secondary reagents. For mouse NKG2D binding assay, cells were incubated with 10 μg/mL of the fusion protein of recombinant soluble mouse NKG2D and human Fc (smNKG2D-Fc; R&D Systems) followed by PE-conjugated $F(ab')_2$ goat anti-human IgG. For H-2K^b expression, cells were incubated with Alex^{647}-conjugated anti-H-2K^b/D^b mAb (Biolegend).

Single-cell suspensions of splenocytes were prepared as described (30). Cells were stained with FITC-conjugated mAb DX5 (eBiosciences) and PE-conjugated anti-mouse NKG2D mAb CX5 (eBiosciences) or A10 (eBiosciences) and analyzed using a BD FACScan or LSRII. For *ex vivo* rsMICB competitive binding assay, freshly isolated splenocytes were incubated with 10 ng/μL rsMICB-FLAG followed with FITC-conjugated mAb M2 (Sigma-Aldrich) and PE-conjugated mAb DX5 (eBiosciences). Data were analyzed using the BD CellQuest^{Pro} (BD Biosciences) or FlowJo software (Tree Star).

Cytotoxicity assay. Fresh NK cells were prepared using Spin^{sep} murine NK enrichment cocktail (Stem Cell Technology) and were >90% DX5$^+$. LAK cells were prepared by culturing NK cells for 4 to 7 days in 1,000 units/mL recombinant human interleukin-2. Cytotoxicity was done in triplicates using the standard 4 h ^{51}Cr release assay (13). Antibody blocking was done by preincubating effector cells with 30 μg/mL NKG2D blocking mAb CX5 (eBiosciences) or preincubating target cells with 100 μg/mL anti-pan RAE-1 polyclonal antibody at 37°C for 1 h (31).

Statistical analysis. Data were analyzed using JMP software. Significance between two animal groups was determined by Student's t test. $P < 0.05$ was considered significant.

Results

Putative cleavage region of MIC(B) in TC2 tumor cells. TC2 is a mouse prostate tumor cell line generated from the TRAMP mouse (27), which does not express any homologous molecules to human MIC (28). TC2 cells were transduced with retroviruses that carry cDNAs of human MICB and GFP. Transduced cells stably expressing high levels of MICB (designated as TC2-MICB cells) were generated by puromycin selection and multiple rounds of flow cytometry cell sorting for GFP-positive cells.

To generate a shedding-resistant form of MICB, we first performed experiments to predict putative cleavage region of MICB by tumor cells. Soluble MICB resulted from TC2 shedding (designated as ssMICB) was immunoprecipitated from supernatant of TC2-MICB cells with a mouse mAb 6D4.6 specific to the α1α2 ectodomain of MICA/B (10). The full-length MICB was immunoprecipitated from cell lysates with the same antibody. Immunocomplexes were separated and immunoblotted with a goat polyclonal antibody AF1599 specific to the ectodomain of MICB. After N-glycosidase (PNGase F) treatment, ssMICB yield two bands of molecular mass ~31 to 33 kDa (Fig. 1A). The molecular mass is consistent with other studies showing soluble MICB and soluble MICA released by human tumor cells (32, 33). When samples were treated with dinitrothiocyanobenzene, a disulfide isomerase inhibitor, only a single band of soluble MICB was revealed (data not shown), suggesting that the two bands of soluble MICB released by TC2 cells are the reduced and nonreduced forms of ssMICB. Similar observation of soluble MICA shed by human tumor cell lines was shown by Kaiser et al. (33). The deglycosylated full-length MICB is shown to be ~41 kDa in the cell lysates (Fig. 1A), consistent with other studies (34). Although the precise cleavage site cannot be determined, these data suggest that MICB was cleaved at the α3 domain proximal to the transmembrane region to generate ssMICB (Fig. 1B). Similar cleavage region is also predicted for human tumor cell lines to generate soluble MICA (33).

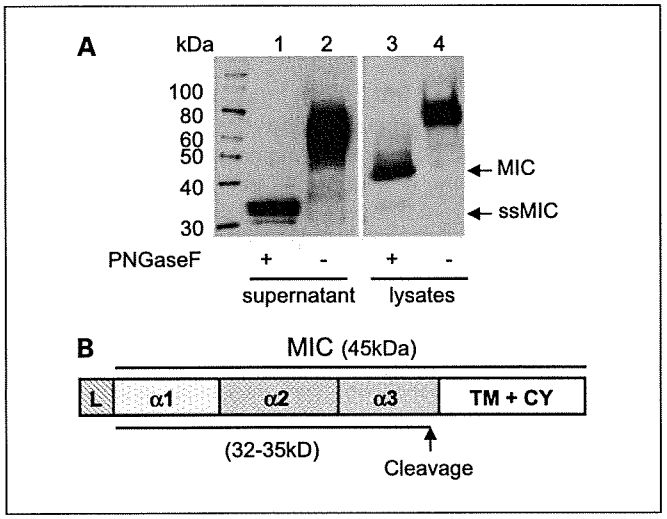

Fig. 1. Putative MICB cleaved site(s) in TC2 cells. *A*, Western blot showing the predicted size of cleaved soluble MICB in TC2 cells. Supernatant and lysates of TC2-MICB cells were immunoprecipitated with anti-MIC mAb 6D4.6. The immunocomplexes were treated with PNGase F and resolved on SDS-PAGE. Proteins were transferred to nitrocellulose membrane and blotted with goat anti-MICB polyclonal antibody. *Lanes 1* and *2*, detection of soluble MICB from TC2-MICB supernatant. The molecular mass of the deglycosylated cleaved soluble MICB is estimated to be 31 to 33 kDa. *Lanes 3* and *4*, detection of full-length MICB from TC2-MICB cell lysates. The full-length deglycosylated MICB is estimated to be 41 kDa on 4% to 15% SDS-PAGE. *B*, putative MICB cleavage site(s).

Generation of tumor cell lines expressing the putative shedding-resistant MICB.A2 and rsMICB. To study the effect of MIC shedding on tumor formation and growth *in vivo*, we generated two forms of MICB, the recombinant secretable form of MICB (rsMICB) and a putative shedding-resistant form of MICB (MICB.A2). rsMICB was generated by deletion of the transmembrane and cytoplasmic domains. MICB.A2 was generated by replacing part of the α3 domain of MICB (amino acids 215-274) with the corresponding residues from HLA-A2 (Fig. 2A). Because NKG2D only interacts with the α1α2 domain of MIC (24), MICB.A2 would presumably continue to recognize NKG2D. rsMICB and MICB.A2 were overexpressed in TC2 cells using the GFP retroviral system described above. Positive-expressing clones were selected by puromycin and repeated sorting by flow cytometry for GFP-positive cells. The expression level of cellular rsMICB and surface MICB.A2 in TC2 cells was confirmed by flow cytometry with the anti-MIC mAb 6D4.6 (Fig. 2B).

Partial replacing the α3 domain of MICB protects from tumor cell shedding. An ELISA assay was used to assess the degree of shedding of MICB and MICB.A2 in TC2 cell lines. Both the capture and the detection antibodies are specific to the extracellular domain of MICB and can also detect MICB.A2 by Western blotting (data not shown). With a given number of cells, the amount of cleaved soluble MIC in the culture supernatant and the amount of MIC in the lysates were

measured by a sandwich ELISA assay (Fig. 2C). The degree of MIC shedding was estimated by the molar percentage of soluble MICB released into the supernatant. Approximately 30% of MICB was cleaved into the medium in TC2 cells, whereas no cleaved form of MICB.A2 was detectable in the culture supernatant (Fig. 2C). This indicates that MICB.A2 cannot be cleaved into soluble forms by tumor cells and is shedding-resistant.

Expression of MICB.A2 in TC2 cells stimulates mouse NK cell cytolytic activity. Human MICB can be recognized by mouse NKG2D and activate mouse NK cells (22, 23). To test whether overexpressing MICB.A2 can also activate mouse NK cells, we first addressed the physical interaction of MICB.A2 with soluble mouse NKG2D-Fc (smNKG2D-Fc) fusion protein by flow cytometry analyses. As measured by mean fluorescence intensity (Fig. 3A), smNKG2D-Fc was more prominently bound by TC2-MICB and TC2-MICB.A2 cells and only weakly bound by TC2 and TC2-rsMICB cells. Accordingly, *in vitro* cytotoxicity assay revealed marked increase in sensitivity of TC2 cells to interleukin-2-activated mouse NK (LAK) cells when MICB or MICB.A2 was overexpressed (Fig. 3B; $P < 0.01$). The increased susceptibility of TC2-MICB and TC2-MICB.A2 cells to LAK cells can be inhibited by preincubation of LAK cells with the NKG2D-specific blocking antibody CX5 (ref. 35; Fig. 3B), suggesting a NKG2D-dependent LAK cell-killing effect. Thus, the shedding-resistant MICB.A2 maintained the functional property of MICB to be recognized by mouse NKG2D.

Although not expressing any MIC homologue, TC2 cells express some levels of endogenous NKG2D ligand RAE-1 variants but not H60 (22, 36). However, the level of endogenous NKG2D ligands is not sufficient to stimulate LAK cell *in vitro* cytotoxicity (Fig. 3B). To address whether the increased

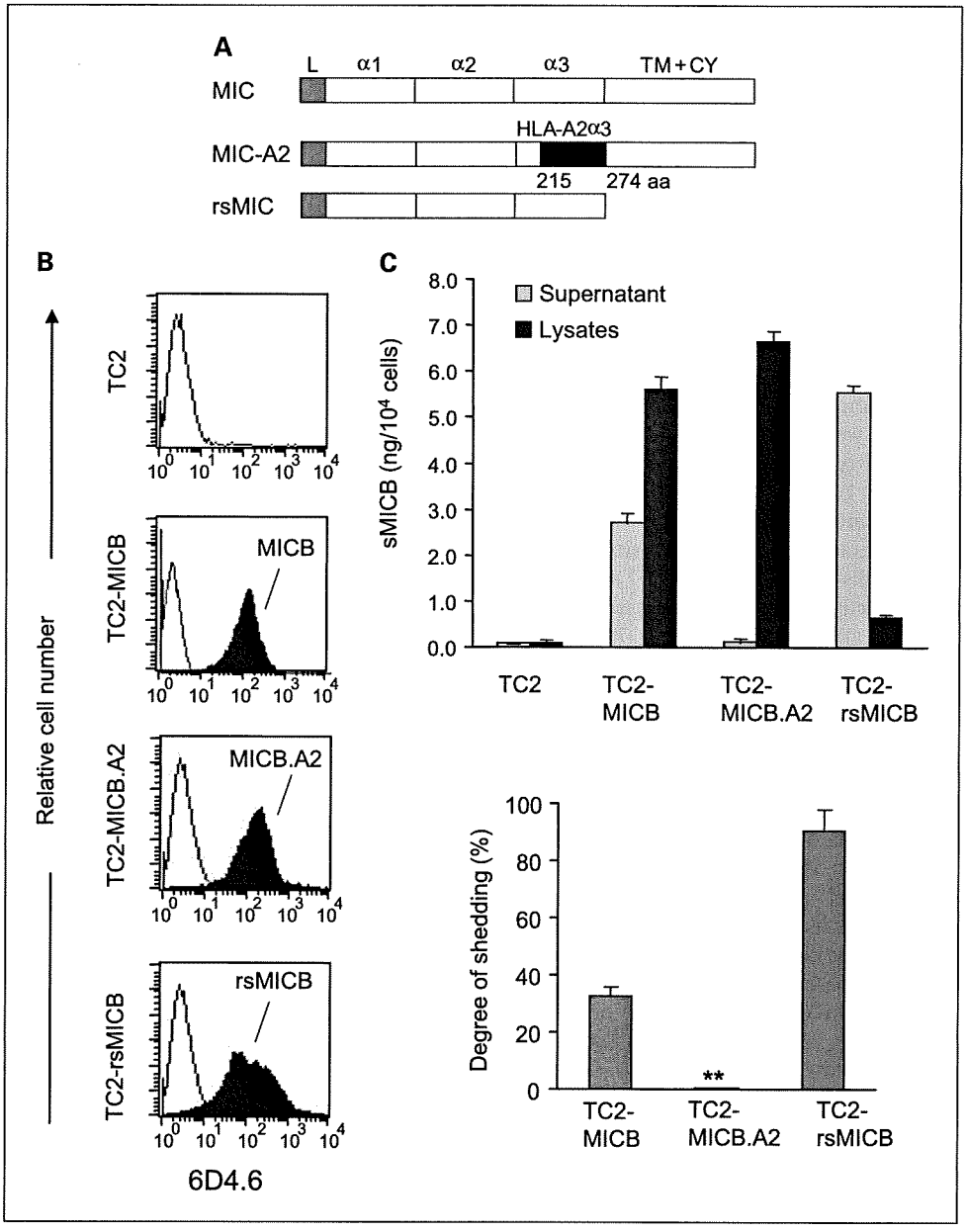

Fig. 2. Construction and expression of the shedding-resistant noncleavable and soluble recombinant forms of MICB (rsMICB) in TC2 cell lines. *A,* generation of the noncleavable form MICB.A2 by replacing amino acids 215 to 274 of the MICB α3 domain with the corresponding sequence of HLA-A2. rsMICB was generated by deletion of the entire transmembrane and cytoplasmic region of MICB. *B,* flow cytometry showing expression levels of MICB, MICB.A2, and rsMICB in TC2 cell lines. cDNAs of MICB, MICB.A2, or rsMICB were inserted into a IRES-GFP retroviral vector pBMNZ. TC2 cells were transduced with respective retrovirus. GFP-positive cells were sorted by flow cytometry. For detection of MICB and MICB.A2 expression, cells were directly incubated with anti-MIC 6D4.6 antibody followed a PE-conjugated secondary reagent. For detection of the secretable rsMICB expression, TC2-rsMICB cells were cultured in the presence of BD GolgiPlug for 3 h to prevent the secretion of rsMICB before harvesting. Cells were resuspended in BD Fixation/Permeabilization solution for 20 min at 4°C and incubated with 6D4.6 followed with a PE-conjugated secondary reagent. *C,* MICB.A2 is shedding-resistant. *Top,* amount of shed soluble MICB in the culture supernatant and MICB in the cell lysates. Cells (4×10^5 per well) were plated on a 6-well plate overnight. Medium was removed and replaced with 1 mL serum-free medium. Six hours later, medium was collected and filtered. Cells were lysed with 1 mL lysis buffer, and 50 μL culture supernatant and cell lysates were used for (s) MICB ELISA assay. *Bars,* SE. *Bottom,* degree of shedding as calculated by molars of soluble MICB in the supernatant versus total molars of soluble MICB and MICB (a sum of supernatant and cell lysates). Final results were normalized by cell numbers at the time of the assay. Results of three independent experiments. *, $P < 0.001$.

sensitivity of TC2-MICB and TC2-MICB.A2 cells to LAK cell killing is possibly due to increased expression of RAE-1, we analyzed endogenous RAE-1 expression on these cell lines by flow cytometry with a rat anti-pan RAE-1 mAb. A consistency of RAE-1 expression among TC2, TC2-MICB, and TC2-MICB.A2 cell lines is shown in Fig. 3C. Furthermore, preincubation of target cells with an anti-pan RAE-1 blocking antibody (30) did not significantly reduce the susceptibility of TC2-MICB or TC2-MICB.A2 cells to LAK cells, whereas the sensitivity of the control RMA-Rae-1β cells to LAK cells was significantly reduced (Fig. 3B). These suggest that the increased killing of TC2-MICB or TC2-MICB.A2 cells by LAK cells is not due to increased RAE-1 expression.

TC2 cells express a very low level of H-2K^b/D^b (37), which is a potential ligand for inhibitory Ly49 receptor families. We analyzed H-2K^b/D^b expression on these cell lines by flow cytometry. Consistent levels of H-2K^b/D^b expression were found in TC2 and cell lines expressing MICB or MICB.A2 (Fig. 3C), suggesting that the increased sensitivity of TC2-MICB and TC2-MICB.A2 cells to LAK cells was not attributed to a reduced level of H-2K^b/D^b expression.

***Shedding-resistant MICB.A2 but not the natural MICB prevents TC2 tumor formation* in vivo.** In three independent experiments, when SCID animals were implanted with TC2-rsMICB, TC2-MICB, or TC2-MICB.A2 cells, none of animals that were implanted with the TC2-MICB.A2 cells developed tumors with a 12-week follow-up observation period, whereas all the animals that were implanted with TC2-rsMICB or TC2-MICB cells developed tumors within 3 weeks (Fig. 4A and B). In addition, no significant difference in tumor growth was observed among TC2, TC2-rsMICB, and TC2-MICB originated tumors (Fig. 4A). To address whether the failure to reject TC2-MICB tumors is due to the large dose (1×10^6) of tumor cells injected, we repeated the experiment with TC2-MICB and TC2-MICB.A2 cells using smaller numbers of inoculated cells. A 10-fold (1×10^5) and a 100-fold (1×10^4) decrease in the number of inoculated tumor cells did not change the outcome (Fig. 4C). We also examined MICB expression in the TC2-MICB-originated tumor cells extracted from SCID animals by flow cytometry. All the extracted tumor cells expressed the similar levels of MICB before implantation (Fig. 4D). This suggests that tumor growth in animals that were implanted with TC2-MICB cells is not due to NK cells selectively eliminating MICB-positive cells.

Shedding of MICB by TC2 cells allows TC2-MICB tumor growth in mice. In 4 h *in vitro* cytotoxicity assays, both TC2-MICB and TC2-MICB.A2 cells were sensitive to LAK cells (Fig. 3B). However, NK tumor immunity was effective only in animals when the noncleavable MICB.A2 was expressed on tumor cells. We propose that the discrepancy of *in vivo* and *in vitro* observation is attributed to tumor cell shedding of MICB *in vivo*, which accumulatively compromises NK cell function in animals implanted with MICB-expressing tumor cells. To test this hypothesis, we measured serum levels of soluble MICB in all the animals 4 weeks after tumor implantation using a sandwich ELISA assay. A significant level of soluble MICB was detected in the sera of animals that were implanted with tumor cells expressing rsMICB and MICB, whereas no soluble MICB was detectable in animals implanted with tumor cells expressing MICB.A2 (Fig. 5A). To address why TC2-MICB cells were sensitive to LAK cell *in vitro*, LAK cells were incubated with the supernatant of TC2-MICB cells for various periods and used as effector cells to kill target TC2-MICB.A2 cells. Only after 8 h incubation, LAK cell-killing ability was significantly affected. Therefore, in the 4 h *in vitro* cytotoxicity assay, the killing ability of LAK cells was not significantly affected by soluble MICB

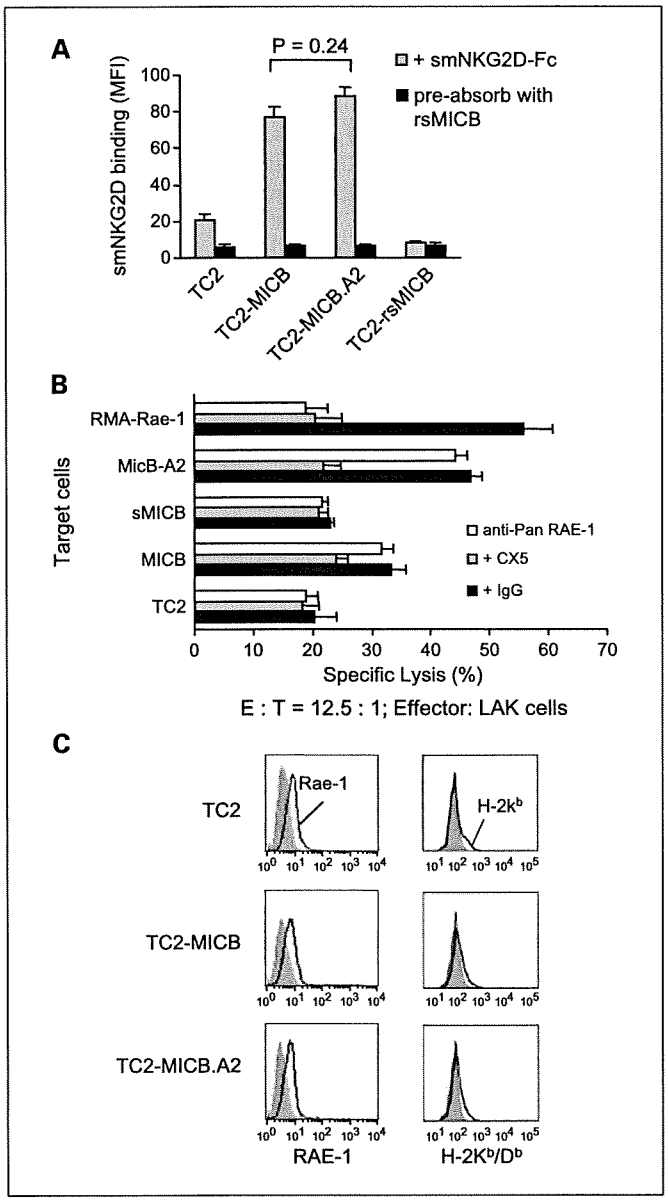

Fig. 3. Overexpression of MICB and MICB.A2 increases the sensitivity of TC2 cells to NK cell killing. *A*, binding of MICB and MICB.A2 by mouse NKG2D. Cells were incubated with the chimeric soluble mouse NKG2D-human Fc (smNKG2D-Fc) followed by PE-conjugated anti-human IgG. Cells were analyzed by flow cytometry. Data are mean fluorescence intensity. When smNKG2D-Fc was preabsorbed with rsMICB, no binding was seen in any of the cell lines. No significant difference was shown in the binding ability between MICB and MICB.A2 ($P = 0.24$). *B*, sensitivity of various MICB-expressing TC2 cells to mouse NK cells. NK cells were isolated from SCID mice and cultured in complete medium with 1,000 units/mL interleukin-2 for 4 d before used as effectors in standard 4 h ^{51}Cr release assay. For blocking NKG2D receptor, effector cells were preincubated with 30 μg/mL CX5 antibody. For blocking RAE-1, target cells were preincubated with 100 μg/mL anti-pan-RAE-1 polyclonal antibody for 1 h before the assay. RMA-Rae-1β cells were used as positive controls for blocking antibodies. *E:T*, effector:target ratio. *Bars*, SE. *, $P < 0.01$, compared with TC2 cells as targets. *C*, flow cytometry histograms showing surface expression of RAE-1 (*left*) and H-2K^b/D^b (*right*) in TC2, TC2-MICB, and TC2-MICB.A2 cells. *Filled histograms*, cells were stained with control isotype antibodies; *open histograms*, cells were stained with specific antibodies. Results of three independent experiments.

resulted from target TC2-MICB cells (data not shown). We further examined NK cell tumor-killing ability from these animals. For this purpose, freshly isolated splenic NK cells were used as effector cells for *in vitro* cytotoxicity assay. NK cells from mice bearing MICB- and rsMICB-expressing tumors had a significant reduction in cytotoxicity against TC2-MICB.A2 target cells in comparison with those from TC2 tumor-bearing or tumor-free animals ($P < 0.01$; Fig. 5B). The cytotoxicity of these NK cells was inhibited by preincubating with a NKG2D-specific inhibitory mAb CX5 (Fig. 5B), suggesting a NKG2D-dependent effect. Together, these results suggest that persistent presence of soluble MICB *in vivo* due to tumor cell shedding of MICB compromised NKG2D-mediated NK cell lytic activity and thus permitted the growth of MICB-expressing tumor cells.

Persistent presence of soluble MICB blocks the NKG2D-mediated NK cell recognition of target cells. When animals were treated with the CX5 antibody to block NKG2D receptor, injection of TC2-MICB.A2 cells gave rise to tumor formation in all the SCID animals (Fig. 6A). This suggests that the inhibition of TC2-MICB.A2 tumor formation in SCID animals is NKG2D-dependent. To test the effect of presence of soluble MICB on tumor formation of MICB.A2-expressing cells, we injected animals with purified rsMICB (50 ng) before and after implanting TC2-MICB.A2 cells. Under this experimental

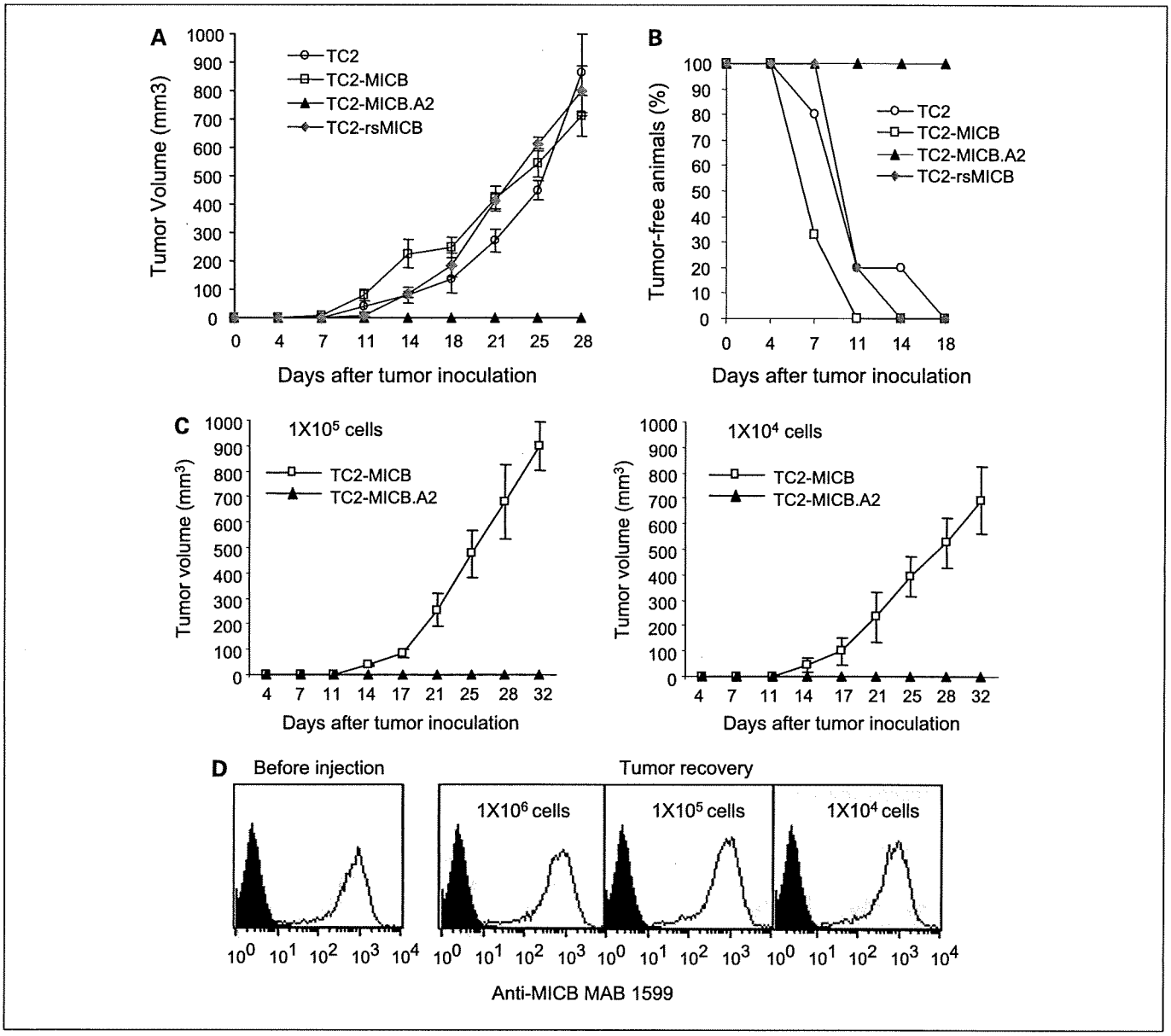

Fig. 4. Expression of MICB.A2 but not the cleavable MICB prevents tumor formation *in vivo*. Six animals were used in each group. Tumor growth was monitored twice weekly. Tumor volume was estimated by the formula: $V = L^2 \times W / 2$. *A,* tumor growth of various MICB-expressing TC2 cells in SCID mice. *B,* rate of tumor formation of various MICB-expressing TC2 cells in SCID mice. Cells (1×10^6) were injected subcutaneously into each animal in *A* and *B*. *C,* tumor growth of TC2-MICB cells when injected at lower doses (1×10^5 and 1×10^4 cells per animal). *D,* representative flow cytometry histoplots showing MICB expression in tumor cells extracted from animals inoculated with TC2-MICB cells compared with prior inoculation. The MICB-specific antibody MAB1599 (R&D Systems) was used as primary antibody. *Filled histogram,* MICB expression in TC2 cells; *open histogram,* MICB expression in TC2-MICB cells or tumor cells. Results of three independent experiments.

condition, implantation of TC2-MICB.A2 cells gave 100% tumor formation (Fig. 6A). Tumor cells extracted from these animals were shown to be GFP-positive and express MICB.A2 by flow cytometry analyses (data not shown). NK cells isolated from these animals showed very little cytolytic activity against TC2-MICB.A2 target cells (data not shown). These data suggest that persistent presence of soluble MICB compromises the cytotoxicity of NK cells against TC2-MICB.A2 cells.

We sought the mechanisms by which tumor shedding-derived soluble MICB would diminish NK cell activity. Soluble MICB may down-modulate surface NKG2D expression on NK cells (16) or block the recognition of NK cells to target cells by physical occupancy of the NKG2D receptor. To distinguish these two mechanisms, we first analyzed NKG2D expression on splenic NK cells freshly isolated from animals injected with various TC2 tumor cells using flow cytometry analyses with a nonblocking NKG2D antibody A10 (29). There was no significant difference in surface NKG2D expression on NK cells from mice bearing TC2-MICB and TC2-rsMICB tumors compared with those from animals bearing TC2 tumors or tumor-free animals (Fig. 6B), suggesting that the suppressive effect of soluble MICB on NK cell activity was not through down-modulation of surface NKG2D receptor. We further examined the occupancy of NKG2D receptor on NK cells by tumor-derived soluble MICB using competitive binding assay. Freshly isolated splenocytes were incubated with purified rsMICB-FLAG, and NK cell-binding ability to rsMICB-FLAG was measured by flow cytometry using the anti-FLAG mAb M2.

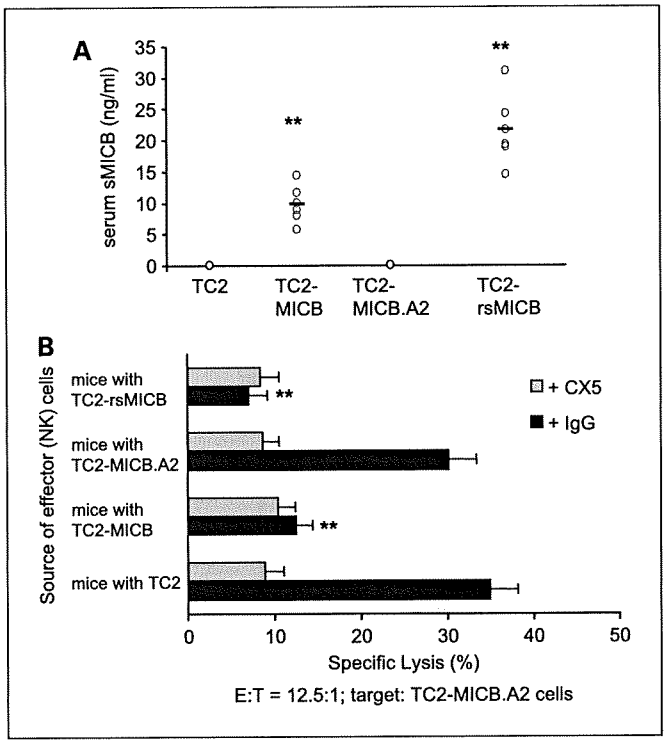

Fig. 5. Shedding of MICB by TC2-MICB cells compromises NK cell activity *in vivo*. *A*, serum levels of soluble MICB in all the tumor-bearing animals. *B*, reduced NKG2D-dependent NK cell cytotoxicity of splenic NK cells from animals bearing TC2-rsMICB and TC2-MICB tumors. Freshly isolated NK cells were used as effectors; TC2-MICB.A2 cells were used as target cells. **, $P < 0.01$, compared with TC2 or TC2-MICB.A2. Results of three independent experiments.

NK cells from animals inoculated with TC2-MICB or TC2-rsMICB cells had significantly reduced binding to rsMICB-FLAG compared with those from animals inoculated with TC2 or TC2-MICB.A2 cells ($P < 0.01$; Fig. 6C). Together, these data suggest that soluble MICB dampens NKG2D-dependent NK cell activity mainly by masking the NKG2D receptor and thus blocking the interaction of NKG2D with target molecules.

Discussion

This study has provided conclusive evidence supporting the hypothesis that shedding of MIC by transformed cells can promote tumor growth. In this study, we generated a shedding-resistant NKG2D ligand MICB.A2 by partially modifying the α3 domain of MICB and showed that overexpressing MICB.A2 prevented tumor formation by the mouse prostate tumor cell line TC2. We also showed that, when soluble MICB was persistently present, expression of the shedding-resistant MICB.A2 on the tumor cell surface did not prevent or delay tumor formation *in vivo*. Our study signifies the effect of MIC shedding on tumor formation and the magnitude of sustained MIC-induced NKG2D immunity in preventing early tumor development.

Although the mechanisms of MIC shedding is still under investigation (19, 33, 38), clinical evidence has shown that shedding of MIC is common in MIC-positive cancers, such as prostate, colon, breast adenocarcinomas, and melanomas (10–13). In these patients, the function of NK and/or CD8 T cells was compromised due to soluble MIC-induced internalization of the NKG2D receptor (13, 16–18). Thus, it was hypothesized that MIC shedding in tumors can promote tumor immune evasion and progress to advanced disease. Recent studies have shown that MIC expression is not restricted in tumor cells and that MIC can be induced in cells in response to DNA damage (39), a prior event to transformation. Therefore, the current study indicates that, in the event of malignant transformation, inhibiting shedding of MIC from MIC-positive transformed cells can prevent the initiation of tumor formation.

We chose to overexpress human MICB rather than mouse NKG2D ligands in this study for the following rationales. Firstly, MIC has been shown to be shed by tumor cells in cancer patients; thus, the study is clinically relevant. Secondly, MICB has been shown to interact with mouse NKG2D, and MICB-positive cells are sensitive to mouse NK cells (22, 23). We also have shown that MICB was shed by the mouse prostate cell line TC2 in the same pattern as MIC shedding in prostate cancer patients.[4] Thirdly, although mouse NKG2D ligands are functionally similar to human MIC in NK cell activation, these molecules are structurally different and may have different physiologic roles. Mouse NKG2D ligands lack the α3 domain and are mostly GPI-linked proteins (9); in addition, little is known about what controls the expression of mouse NKG2D ligands *in vivo* and whether they would shed in a similar fashion to MIC in human tumor cells. Lastly, different from human NKG2D ligands, studies have shown that naturally expressed mouse NKG2D ligands on tumor cells may not cause tumor rejection largely due to insufficient levels of the ligand expression (2) or low affinity of binding to NKG2D (40). In

[4] Wu, unpublished data.

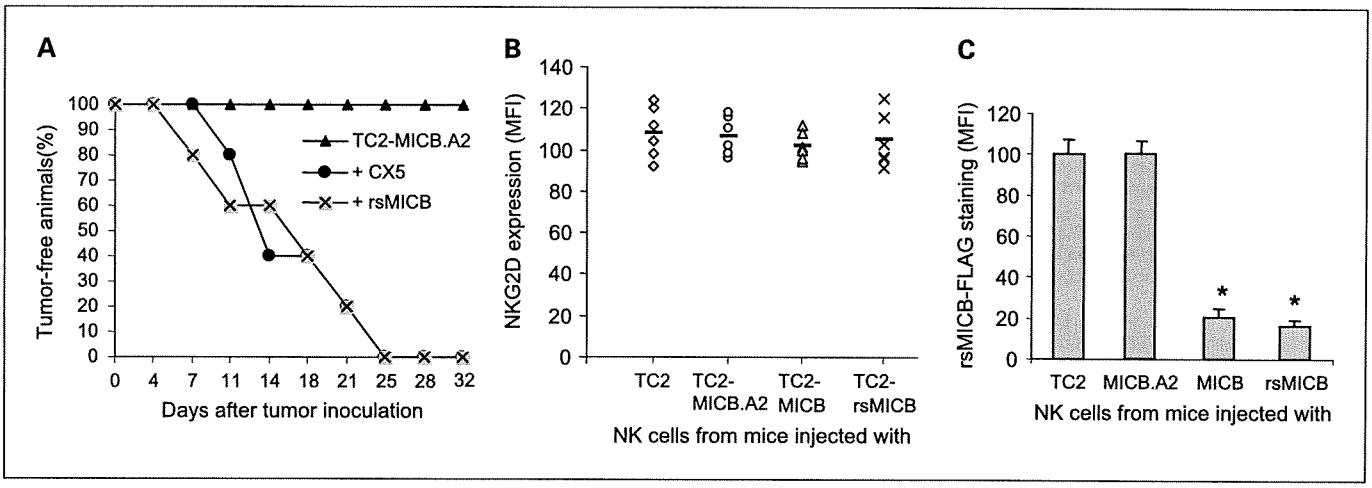

Fig. 6. Soluble MICB-induced NK cell dysfunction. *A, in vivo* blocking NKG2D with CX5 antibody or neutralization the function of NKG2D with rsMICB enables TC2-MICB.A2 cells to form tumors. To block NKG2D receptor *in vivo*, 100 μg NKG2D-specific antibody CX5 was injected intraperitoneally on the day before and the day after tumor implantation and thereafter every 3 d. To modify NKG2D function, animals were intraperitoneally injected with 50 ng purified rsMICB before implantation of TC2-MICB.A2 cells and thereafter twice a week for 4 wk. *B,* measurements of NKG2D expression shown as mean fluorescence intensity on splenic NK cells freshly isolated from SCID animals ($n = 6$) injected with various tumor cells. *Columns,* mean fluorescence intensity. *C,* competitive binding assay indicating saturation of NKG2D receptor by soluble MICB in animals bearing TC2-MICB and TC2-rsMICB tumors. Freshly isolated splenocytes were incubated with 10 ng/μL rsMICB-FLAG followed by FITC-conjugated anti-FLAG mAb M2 and PE-conjugated mAb DX5. Data are measurements of mean fluorescence intensity of M2 staining from six animals of each experimental group. *Bars,* SE. *, $P < 0.01$, compared with animals injected with TC2 or TC2-MICB.A2 tumor cells.

this study, although TC2 cells express some levels of mouse NKG2D ligand RAE-1 variants, TC2 tumors were palpable in SCID mice within 1 week after implantation and grew aggressively (Fig. 4), suggesting that the levels of activating RAE-1 variants expressed by TC2 cells are too low to induce antitumor immunity. This was also supported by the low binding ability of soluble mouse NKG2D to TC2 cells (Fig. 3A). Therefore, it could be challenging to define an optimal level of mouse NKG2D ligand expression for tumor rejection. Together, the choice of MICB makes the *in vivo* study described here more clinically relevant to human cancers.

In activated mouse NK cells, due to alternative DNA splicing, two isoforms of NKG2D couple with two intracellular adaptors, DAP10 and DAP12, which trigger phosphatidylinositol 3-kinase and Syk family protein tyrosine kinase, respectively (40, 41). In human, NKG2D only associates with DAP10. However, in mouse NK cells lacking DAP12 or Syk family kinases, DAP10-phosphatidylinositol 3-kinase pathway alone is sufficient to initiate ligand-induced NKG2D-mediated killing of target cells (41). Thus, regardless that signaling via mouse NKG2D is more complex than human NKG2D, effect of NKG2D ligand shedding on tumor formation as found in the current study would be significant in both species.

Most of the *in vitro* evidence suggests that engagement of tumor cell surface MIC to NKG2D can activate NK cell immunity against tumor cells. Thus, expression of MIC on tumor cells is proposed to activate host protective antitumor immunoresponse. However, most of the epithelial originated human cancer cells were found to have MIC expressed on the surface, suggesting the ineptness of MIC-induced NK cell immunity. Consistent with clinical observations, we also show that overexpressing the natural cleavable form of MICB in TC2 cells has no significant effect on tumor growth *in vivo*. Although overexpressing the noncleavable shedding-resistant MICB.A2 can cause TC2 tumor rejection, this effect can be inhibited by the persistent presence of soluble MICB (Fig. 6A). Together, our data suggest that the role of MIC in host tumor immunosurveillance is determined by whether MIC is all or partially membrane-bound. If all the MIC molecules sustain to be membrane-bound and noncleavable, expression of MIC activates NK cell-mediated host immunity. In contrast, if a portion of the MIC molecules is cleaved and becomes soluble, tumor cells cannot be targeted by NK cells due to soluble MIC-mediated masking and possible down-regulation of the receptor NKG2D regardless of abundant MIC remaining on the tumor cell surface as observed in many cancer patients (10–13).

In summary, our data provide the first *in vivo* conclusive evidence of the effect of MIC shedding on tumor growth and the importance of sustained MIC ligand-NKG2D receptor interaction in control of tumor growth. In addition, our results show no significant difference in tumor growth among animals whether the natural form of MICB or soluble recombinant MICB was expressed. This observation implies that wild-type MIC expression in established tumors may have very little effect on inducing host NK cell activation due to shedding of MIC by tumor cells and the consequent dampening of host immunity. Together, our results suggest that strategies to sustain the recognition of NKG2D receptor and tumor MIC ligand may have potential anticancer therapeutic implications.

Disclosure of Potential Conflicts of Interest

No potential conflicts of interest were disclosed.

Acknowledgments

We thank Michael Tao for assistance with animal tissue collections and Dr. Norman M. Greenberg for helpful discussions.

References

1. Cerwenka A, Bakker AB, McClanahan T, et al. Retinoic acid early inducible genes define a ligand family for the activating NKG2D receptor in mice. Immunity 2000; 12:721–7.
2. Diefenbach A, Jensen ER, Jamieson AM, Raulet DH. Rae1 and H60 ligands of the NKG2D receptor stimulate tumour immunity. Nature 2001;413:165–71.
3. Cerwenka A, Baron JL, Lanier LL. Ectopic expression of retinoic acid early inducible-1 gene (RAE-1) permits natural killer cell-mediated rejection of a MHC class I-bearing tumor *in vivo*. Proc Natl Acad Sci U S A 2001; 98:11521–6.
4. Diefenbach A, Hsia JK, Hsiung MY, Raulet DH. A novel ligand for the NKG2D receptor activates NK cells and macrophages and induces tumor immunity. Eur J Immunol 2003;33:381–91.
5. Carayannopoulos LN, Naidenko OV, Fremont DH, Yokoyama WM. Cutting edge: murine UL16-binding protein-like transcript 1: a newly described transcript encoding a high-affinity ligand for murine NKG2D. J Immunol 2002;169:4079–83.
6. Smyth MJ, Swann J, Cretney E, Zerafa N, Yokoyama WM, Hayakawa Y. NKG2D function protects the host from tumor initiation. J Exp Med 2005;202:583–8.
7. Long EO. Tumor cell recognition by natural killer cells. Semin Cancer Biol 2002;12:57–61.
8. Raulet DH. Roles of the NKG2D immunoreceptor and its ligands. Nat Rev Immunol 2003;3:781–90.
9. Cerwenka A, Lanier LL. NKG2D ligands: unconventional MHC class I-like-molecules exploited by viruses and cancer. Tissue Antigens 2003;61:335–43.
10. Groh V, Rhinehart R, Secrist H, Bauer S, Grabstein KH, Spies T. Broad tumor-associated expression and recognition by tumor-derived γδ T cells of MICA and MICB. Proc Natl Acad Sci U S A 1999;96:6879–84.
11. Vetter CS, Groh V, thor Straten P, Spies T, Brocker EB, Becker JC. Expression of stress-induced MHC class I related chain molecules on human melanoma. J Invest Dermatol 2002;118:600–5.
12. Jinushi M, Takehara T, Tatsumi T, et al. Expression and role of MICA and MICB in human hepatocellular carcinomas and their regulation by retinoic acid. Int J Cancer 2003;104:354–61.
13. Wu JD, Higgins LM, Steinle A, Cosman D, Haugk K, Plymate SR. Prevalent expression of the immunostimulatory MHC class I chain-related molecule is counteracted by shedding in prostate cancer. J Clin Invest 2004;114:560–8.
14. Friese MA, Platten M, Lutz SZ, et al. MICA/NKG2D-mediated immunogene therapy of experimental gliomas. Cancer Res 2003;63:8996–9006.
15. Busche A, Goldmann T, Naumann U, Steinle A, Brandau S. Natural killer cell-mediated rejection of experimental human lung cancer by genetic overexpression of major histocompatibility complex class I chain-related gene A. Hum Gene Ther 2006;17: 135–46.
16. Groh V, Wu J, Yee C, Spies T. Tumour-derived soluble MIC ligands impair expression of NKG2D and T-cell activation. Nature 2002;419:734–8.
17. Doubrovina ES, Doubrovin MM, Vider E, et al. Evasion from NK cell immunity by MHC class I chain-related molecules expressing colon adenocarcinoma. J Immunol 2003;171:6891–9.
18. Raffaghello L, Prigione I, Airoldi I, et al. Downregulation and/or release of NKG2D ligands as immune evasion strategy of human neuroblastoma. Neoplasia 2004;6:558–68.
19. Salih HR, Rammensee HG, Steinle A. Cutting edge: down-regulation of MICA on human tumors by proteolytic shedding. J Immunol 2002;169: 4098–102.
20. Holdenrieder S, Stieber P, Peterfi A, Nagel D, Steinle A, Salih HR. Soluble MICA in malignant diseases. Int J Cancer 2006;118:684–7.
21. Marten A, von Lilienfeld-Toal M, Buchler MW, Schmidt J. Soluble MIC is elevated in the serum of patients with pancreatic carcinoma diminishing γδ T cell cytotoxicity. Int J Cancer 2006;119:2359–65.
22. Diefenbach A, Jamieson AM, Liu SD, Shastri N, Raulet DH. Ligands for the murine NKG2D receptor: expression by tumor cells and activation of NK cells and macrophages. Nat Immunol 2000;1:119–26.
23. Dunn C, Chalupny NJ, Sutherland CL, et al. Human cytomegalovirus glycoprotein UL16 causes intracellular sequestration of NKG2D ligands, protecting against natural killer cell cytotoxicity. J Exp Med 2003;197:1427–39.
24. Li P, Morris DL, Willcox BE, Steinle A, Spies T, Strong RK. Complex structure of the activating immunoreceptor NKG2D and its MHC class I-like ligand MICA. Nat Immunol 2001;2:443–51.
25. Holmes MA, Li P, Petersdorf EW, Strong RK. Structural studies of allelic diversity of the MHC class I homolog MIC-B, a stress-inducible ligand for the activating immunoreceptor NKG2D. J Immunol 2002; 169:1395–400.
26. Strong RK. Asymmetric ligand recognition by the activating natural killer cell receptor NKG2D, a symmetric homodimer. Mol Immunol 2002;38: 1029–37.
27. Foster BA, Gingrich JR, Kwon ED, Madias C, Greenberg NM. Characterization of prostatic epithelial cell lines derived from transgenic adenocarcinoma of the mouse prostate (TRAMP) model. Cancer Res 1997;57:3325–30.
28. Bahram S, Spies T. Nucleotide sequence of a human MHC class I MICB cDNA. Immunogenetics 1996;43: 230–3.
29. Horton RM, Cai ZL, Ho SN, Pease LR. Gene splicing by overlap extension: tailor-made genes using the polymerase chain reaction. Biotechniques 1990;8: 528–35.
30. Ho EL, Carayannopoulos LN, Poursine-Laurent J, et al. Costimulation of multiple NK cell activation receptors by NKG2D. J Immunol 2002;169:3667–75.
31. Masuda H, Saeki Y, Nomura M, et al. High levels of RAE-1 isoforms on mouse tumor cell lines assessed by anti-"pan" RAE-1 antibody confer tumor susceptibility to NK cells. Biochem Biophys Res Commun 2002; 290:140–5.
32. Salih HR, Goehlsdorf D, Steinle A. Release of MICB molecules by tumor cells: mechanism and soluble MICB in sera of cancer patients. Hum Immunol 2006; 67:188–95.
33. Kaiser BK, Yim D, Chow IT, et al. Disulphide-isomerase-enabled shedding of tumour-associated NKG2D ligands. Nature 2007;447:482–6.
34. Wu J, Chalupny NJ, Manley TJ, Riddell SR, Cosman D, Spies T. Intracellular retention of the MHC class I-related chain B ligand of NKG2D by the human cytomegalovirus UL16 glycoprotein. J Immunol 2003;170:4196–200.
35. Ogasawara K, Hamerman JA, Hsin H, et al. Impairment of NK cell function by NKG2D modulation in NOD mice. Immunity 2003;18:41–51.
36. Diefenbach A, Raulet DH. The innate immune response to tumors and its role in the induction of T-cell immunity. Immunol Rev 2002;188:9–21.
37. Grossmann ME, Wood M, Celis E. Expression, specificity and immunotherapy potential of prostate-associated genes in murine cell lines. World J Urol 2001;19:365–70.
38. Le Maux Chansac B, Misse D, Richon C, et al. Potentiation of NK cell-mediated cytotoxicity in human lung adenocarcinoma: role of NKG2D-dependent pathway. Int Immunol 2008;20:801–10.
39. Gasser S, Orsulic S, Brown EJ, Raulet DH. The DNA damage pathway regulates innate immune system ligands of the NKG2D receptor. Nature 2005;436: 1186–90.
40. Diefenbach A, Tomasello E, Lucas M, et al. Selective associations with signaling proteins determine stimulatory versus costimulatory activity of NKG2D. Nat Immunol 2002;3:1142–9.
41. Zompi S, Hamerman JA, Ogasawara K, et al. NKG2D triggers cytotoxicity in mouse NK cells lacking DAP12 or Syk family kinases. Nat Immunol 2003;4: 565–72.

Supplemental Material can be found at:
http://www.jbc.org/cgi/content/full/M804259200/DC1

THE JOURNAL OF BIOLOGICAL CHEMISTRY VOL. 284, NO. 2, pp. 807–817, January 9, 2009

Riplet/RNF135, a RING Finger Protein, Ubiquitinates RIG-I to Promote Interferon- Induction during the Early Phase of Viral Infection* s

Received for publication, June 3, 2008, and in revised form, November 10, 2008 Published, JBC Papers in Press, November 18, 2008, DOI 10.1074/jbc.M804259200

Hiroyuki Oshiumi‡, Misako Matsumoto‡, Shigetsugu Hatakeyama§, and Tsukasa Seya‡1
From the ‡Department of Microbiology and Immunology and the §Department of Biochemistry, Hokkaido University Graduate School of Medicine, Kita-15, Nishi-7, Kita-ku Sapporo 060-8638, Japan

RIG-I (retinoic acid-inducible gene-I), a cytoplasmic RNA helicase, interacts with IPS-1/MAVS/Cardif/VISA, a protein on the outer membrane of mitochondria, to signal the presence of virus-derived RNA and induce type I interferon production. Activation of RIG-I requires the ubiquitin ligase, TRIM25, which mediates lysine 63-linked polyubiquitination of the RIG-I N-terminal CARD-like region. However, how this modification proceeds for activation of IPS-1 by RIG-I remains unclear. Here we identify an alternative factor, Riplet/RNF135, that promotes RIG-I activation independent of TRIM25. The Riplet/RNF135 protein consists of an N-terminal RING finger domain, C-terminal SPRY and PRY motifs, and shows sequence similarity to TRIM25. Immunoprecipitation analyses demonstrated that the C-terminal helicase and repressor domains of RIG-I interact with the Riplet/RNF135 C-terminal region, whereas the CARD-like region of RIG-I is dispensable for this interaction. Riplet/RNF135 promotes lysine 63-linked polyubiquitination of the C-terminal region of RIG-I, modification of which differs from the N-terminal ubiquitination by TRIM25. Overexpression and knockdown analyses revealed that Riplet/RNF135 promotes RIG-I-mediated interferon- promoter activation and inhibits propagation of the negative-strand RNA virus, vesicular stomatitis virus. Our data suggest that Riplet/RNF135 is a novel factor of the RIG-I pathway that is involved in the evoking of human innate immunity against RNA virus infection, and activates RIG-I through ubiquitination of its C-terminal region. We infer that a variety of RIG-I-ubiquitinating molecular complexes sustain RIG-I activation to modulate RNA virus replication in the cytoplasm.

Cytoplasmic viral RNA sensors induce production of type I interferon (IFN)[2] (1, 2). Representative cytoplasmic sensors, RIG-I-like receptors (RLRs) of RIG-I, MDA5, and LGP2, belong to the DEA(D/H) box RNA helicase family (3–6). RIG-I recognizes the 5 end triphosphate of the virus RNA genome or double-stranded RNA (6–8) to sense infection by various RNA viruses (3, 5). The RIG-I protein consists of two N-terminal CARD-like domains, an RNA helicase region and a repressor domain (RD) (9). After recognition of positive or negative single-stranded viral RNA, RIG-I interacts with its adaptor molecule IPS-1/MAVS/Cardif/VISA leading to type I IFN production, thereby protecting host cells from amplified viral replication (10–13). However, only a few copies of viral RNAs usually penetrate the cell membrane to enter the cell at an early infection, and these RLRs are barely present in intact as well as early virus-infected cells (6). The early viral RNA recognition facility should be different from that of the late phase when RIG-I protein is abundant in the cytoplasm and easily re-organizes the virus RNAs. What molecular mechanism is responsible for initial sensing of viral RNA thus remains unknown.

Other RLRs, MDA5 and LGP2, are structurally similar to RIG-I in their having the helicase domain (5, 14). However, MDA5 lacks the RD domain although it possesses CARD-like region at the N terminus like RIG-I. LGP2 does not have a CARD-like region but possesses RD at its C terminus (9). RIG-I and MDA5 recognize different kinds of RNA viruses and in some cases play a redundant role in sensing virus infection, such as influenza B (15). In contrast, LGP2 rather negatively regulates virus replication. LGP2 expression suppressed RIG-I or MDA5 signaling (14, 16), and *lgp2* gene disruption conferred high susceptibility to virus infection on mice (4).

Recently, the majority of proteins involved in the type I IFN-inducing system were found ubiquitinated. For example, the tumor necrosis factor receptor-associated family members, TRAF3 and TRAF6, are ubiquitin ligases to induce ubiquitination of proteins and implicated in activation of IFN regulatory factor (IRF) 3 or nuclear factor (NF) B (13, 17–19). In contrast, a deubiquitinating enzyme, DUBA or A20, suppresses these signals (19, 20). In addition to ubiquitin, ubiquitin-like protein, ISG15, is also conjugated to proteins involved in the IFN-inducing pathway (21, 22). Recent studies have revealed that viral RNA sensors are also ubiquitinated. TRIM25 (ZNF147 or EFP), a member of the ubiquitin-protein isopeptide ligase family, which possesses a RING finger domain, ubiquitinates the

* This work was supported in part by grants-in-aid from the Ministry of Education, Science and Culture of Japan, Ministry of Health, Labour, and Welfare, The Mitsubishi Foundation, and The Mochida Memorial Foundation. The costs of publication of this article were defrayed in part by the payment of page charges. This article must therefore be hereby marked "advertisement" in accordance with 18 U.S.C. Section 1734 solely to indicate this fact.

s The on-line version of this article (available at http://www.jbc.org) contains supplemental Figs. S1–S6.

The nucleotide sequence(s) reported in this paper has been submitted to the GenBank™/EBI Data Bank with accession number(s) AB470605.

1 To whom correspondence should be addressed: Dept. of Microbiology and Immunology, Graduate School of Medicine, Hokkaido University, Kita-ku, Sapporo 060-8638, Japan. Tel.: 81-11-706-5073; Fax: 81-11-706-7866; E-mail: seya-tu@pop.med.hokudai.ac.jp.

2 The abbreviations used are: IFN, interferon; RT, reverse transcription; RLR, RIG-I-like receptor; HA, hemagglutinin; siRNA, small interference; m.o.i., multiplicity of infection; VSV, vesicular stomatitis virus; IRF, IFN regulatory factor; Ub, ubiquitin; ORF, open reading frame; RD, repressor domain.

CARD-like domains of RIG-I thereby facilitating the RIG-I-mediated activation of type I IFN signaling (23, 24), although Shimotohno and co-workers (25) previously reported that TRIM25 (EFP) does not polyubiquitinate the RIG-I CARD-like region as far under their conditions. Expression of TRIM25 increases RIG-I CARD-like region-mediated signaling; however, it remains to be determined whether the activation of full-length RIG-I requires other ubiquitin ligase (23). Another ubiquitin ligase RNF125 mediates lysine 48-linked polyubiquitination of RIG-I, which leads to degradation of RIG-I through the proteasome (25).

Here we examined what molecular complex participates in an early RIG-I-mediated RNA recognition and IFN signaling by yeast two-hybrid screening. Here we detected two novel RING finger proteins that bound to RIG-I, and we found that one, RNF135, facilitated RIG-I-mediated type I IFN induction via ubiquitinating RIG-I. RNF135 plays a crucial role in the RIG-I response to minimal copies of viral RNA, and by binding to the C-terminal helicase and RD regions of RIG-I, RNF135 facilitates RIG-I C-terminal ubiquitination to up-regulate RIG-I-mediated IFN signaling and suppress viral replication. Hence, we renamed it as RNF135 Riplet (RING finger protein leading to RIG-I activation). To our knowledge, this is the first study demonstrating that C-terminal ubiquitination of RIG-I is important for full IFN induction by RIG-I.

EXPERIMENTAL PROCEDURES

Cell Cultures—HEK293 and Vero cells were cultured in Dulbecco's modified Eagle's medium with 10% fetal calf serum (Invitrogen), and HeLa cells were in minimum Eagle's medium with 2 mM L-glutamine and 10% fetal calf serum (JRH Biosciences). HEK293FT cells were maintained in Dulbecco's modified Eagle's high glucose medium containing 10% heat-inactivated fetal calf serum (Invitrogen).

Plasmids—cDNA fragment encoding a C-terminal region of Riplet was isolated by yeast two-hybrid screening using human lung cDNA library. The 5 region encoding the remaining N-terminal region was amplified by PCR using primers Riplet-F1 and Riplet-R1, and human lung cDNA library was used for its template. Two cDNA fragments, which cover the entire ORF of Riplet, were joined by PCR using primers Riplet-F1, R1, F2, and R2 and then inserted into pCR-blunt vector (Invitrogen). The primers sequences are as follows: F1, GCCTCGAGGCCACCATGGCGGGCCTGGGCCTGGG; R1, CGGCCAGGTCCTGCAGTAGC; F2, GCACCTGCGGAAGAACACGC; and R2, GGGGATCCCACCTTTACTTGCTTTATTATCAGG. The obtained cDNA was cloned into XhoI-NotI restriction sites of pEF-BOS expression vector, and the HA tag was fused at the C-terminal end of Riplet. Riplet-DN (dominant negative) expression vector was constructed by amplifying the relevant Riplet cDNA fragment using the primers Riplet-X-F-C and Riplet-R2 and subcloned into pEF-BOS. The primer sequence of Riplet-X-F-C was as follows: GCTCGAGGCCACCATGCCGCACCTGCGGAAGAACACGC. Riplet-L248fs expression vector was made by deleting 1 base at position 742 by standard PCR-mediated site-directed mutagenesis methods with primers Riplet-L248fs-F and Riplet-L248fs-R as follows: Riplet-L248fs-F, CCAGAGCCACCCTGCATCAGGAGAGCTTCTCGG, and Riplet-L248fs-R, CCGAGAAGCTCTCCTGATGCAGGGTGGCTCTGG. All cloned *RIPLET* cDNA fragments were sequenced, and it was confirmed that there were no mutations. Full-length RIG-I expressing vector, Gal4-IRF-3, Gal4-DBD, and p55 UASG-Luc reporter plasmids were gifts from Dr. T. Fujita (Kyoto University, Kyoto, Japan). p125 luc reporter plasmid was a gift from Dr. T. Taniguchi (University of Tokyo, Tokyo, Japan). RIG-I RD expressing vector was made with primers RIG-I RD-F and RIG-I RD-R; the RIG-I dRD cDNA fragment, which encodes ORF of RIG-I from the 1- to 754-amino acid region, was made by using primers RIG-I-(1–754)F and RIG-I-(1–754)R. The obtained cDNA fragments were sequenced, and it was confirmed that there were no mutations caused by PCR. The primers sequences are as follows: RIG-I RD-F, GAT GAT AAA GGT ACC ACC GGT AGC AAG TGC TTC CTT CTG; RIG-I RD-R, AAG GAA GCA CTT GCT ACC GGT GGT ACC TTT ATC ATC ATC ATC; RIG-I-(1–754)F, GC AGA GGA AGA GCA AGA TGA TAT CAG GTC CTC AAT CTT C; and RIG-I-(1–754)R, ATT GAG GAC CTG ATA TCA TCT TGC TCT TCC TCT GCC TC.

Northern Blotting—Human *RIPLET* 1092-bp cDNA fragment (208–1299) was used for the probe for Northern blotting. The Northern blot membranes, human 12-lane MTN blot and MTN blot III, were purchased from Clontech. The homology of human *RIPLET* and *TRIM25* in the probe region was 46%. We used a stringent condition for Northern blotting to exclude the cross-hybridization between the *RIPLET* and *TRIM25* genes. Briefly, the probe was labeled with [-^{32}P]dCTP using Rediprime II Random Prime labeling system (GE Healthcare). The labeled probe was hybridized to the membrane with ExpressHyb hybridization solution (Clontech) at 68 °C for 1 h. The membrane was washed with washing solution I (2 SSC, 0.05% SDS) for 40 min, and then washed with washing solution II (0.1 SSC, 0.1% SDS) for 40 min. Riplet mRNA bands were detected with x-ray film.

Reporter Gene Analysis—HEK293 cells were transiently transfected in 24-well plates using FuGENE HD (Roche Applied Science) with expression vectors, reporter plasmids, and internal control plasmid coding *Renilla* luciferase. The total amounts of plasmids were normalized with empty vector. For poly(I-C) stimulation, 24 h after transfection, cells were stimulated with medium containing poly(I-C) (50 g/ml) and DEAE-dextran (0.5 mg/ml) for 1 h, and then the medium was exchanged with normal medium and incubated for an additional 3 h. Cells were lysed with lysis buffer (Promega) and luciferase, and *Renilla* luciferase activities were measured by the dual luciferase assay kit (Promega). Relative luciferase activities were calculated by normalizing luciferase activity by *Renilla* luciferase activity, and dividing the normalized value by control in which only empty vector, reporter, and internal control plasmid were transfected. Values are expressed as mean relative stimulations S.D. for a representative experiment, and each was performed three times in duplicate (unless otherwise indicated in the legends).

RNA Interference—Reporter and siRNA (20 nM final concentration) for Riplet or control were transfected into HEK293 cells with Lipofectamine 2000 (Invitrogen) by the standard method described in the manufacturer's protocol. Empty vec-

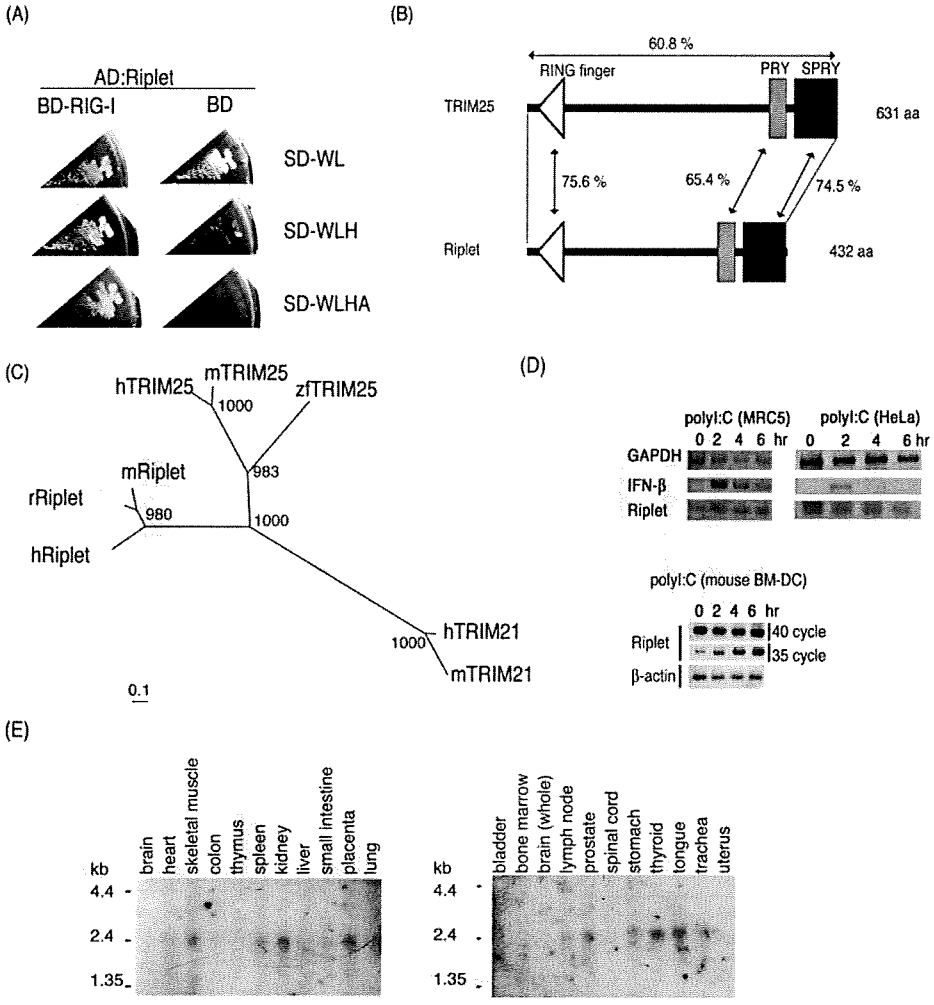

FIGURE 1. Isolation of Riplet by yeast two-hybrid screening. A, yeast cells carrying both RIG-I and Riplet can grow in selective media (SD-WLH, SD-WLHA), whereas yeast cells carrying RIG-I alone only grow in nonselective media (SD-WL), indicating the physical interaction of RIG-I with Riplet. B, human Riplet protein sequence is 60.8% identical to human TRIM25. The RING finger domains and SPRY motifs show higher sequence similarities between the two proteins. aa, amino acids. C, phylogenetic tree constructed by the Neighbor-Joining method shows that Riplet is similar to TRIM25. h, m, r, or zf represent human, mouse, rat, or zebrafish, respectively. The numbers on the node are bootstrap probabilities (n 1000). D, HeLa cell, human primary-cultured fibroblast cell, MRC5, or bone marrow-derived mouse dendritic cell (BM-DC) were stimulated with poly(I-C) (50 g/ml) for indicated hours. Total RNA was extracted with TRIzol reagent, and then RT-PCR was carried out using primers shown under "Experimental Procedures." GAPDH, glyceraldehyde-3-phosphate dehydrogenase. E, Northern blot membranes containing 1 g of poly(A) RNA per lane from human tissues were blotted with human Riplet probe.

tor was added to normalize the final plasmid amount. 48 h after transfection, cells were stimulated with poly(I-C) for 4 h. For VSV infection, 24 h after transfection, cells were infected with VSV at m.o.i. 1, and cell lysate was prepared after 12 h for reporter gene assays. The degree of gene silencing was confirmed by RT-PCR using RNA extracted from cells 24 h after transfection. PCR primers used for the RT-PCR were Riplet-F3 (ACTGGGAAGTGGACACTAGG) and Riplet-R3 (ACTCATACAGAAGCTTCTCC). siRNAs were purchased from Funakoshi Co., Ltd. (Tokyo Japan), and the siRNA sequences of Riplet siRNA were GACUAUGGACUCUUGUUGUGU (sense) and ACAACAAGAGUCCAUAGUCCU (antisense). Control siRNA sequences were CUGUUGGUUUAGUAAGCCUGU (sense) and AGGCUUACUAAACCAACAGUC (antisense). Another siRNA, Riplet si-1, and control negative siRNA (silencer negative control 1 siRNA, AM4611) were purchased from Applied Biosystems. siRNA sequences were Riplet si-1 GGGAAAGCUUGCCUUCUAUdTdT (sense) and AUAGAAGGCAAGCUUUCCCdTdC (antisense).

Virus Preparation and Infection—VSV Indiana strain and poliovirus were amplified using Vero cells. HEK293 cells were transfected in 24-well plates with plasmid encoding *RIG-I*, Riplet, or no insert. 24 h after transfection, cells were infected with viruses for 24 h, and the titers of virus in culture supernatant were measured by plaque assay using Vero cells. For RNA interference assay, cells were transfected with siRNA with Lipofectamine 2000. 24 h after transfection, cells were infected with viruses at m.o.i. 0.001 for 18 h, and the titer in culture supernatant were determined by plaque assay.

Immunoprecipitation—HEK293FT cells were transfected in 6-well plates with plasmids encoding FLAG-tagged RIG-I and/or HA-tagged Riplet. The plasmid amounts were normalized by the addition of empty plasmid. 24 h after transfection, cells were lysed with lysis buffer (20 mM Tris-HCl (pH 7.5), 125 mM NaCl, 1 mM EDTA, 10% glycerol, 1% Nonidet P-40, 30 mM NaF, 5 mM Na_3VO_4, 20 mM iodoacetamide, and 2 mM phenylmethylsulfonyl fluoride), and then proteins were immunoprecipitated with rabbit anti-HA polyclonal (Sigma) or anti-FLAG M2 monoclonal antibody (Sigma). The precipitated samples were analyzed by SDS-PAGE and stained with anti-HA (HA1.1) (Covance) or anti-FLAG M2 monoclonal antibody. For ubiquitination assay of RIG-I, the plasmid encoding two multiple HA-tagged ubiquitins was used. HEK293FT cells were transfected with plasmids encoding FLAG-tagged RIG-I, Riplet, or 2 HA-tagged ubiquitin. 24 h after transfection, cells were lysed, and then RIG-I was immunoprecipitated as described above. The samples were analyzed by SDS-PAGE and stained with anti-HA polyclonal antibody (for detection of ubiquitination) or anti-FLAG monoclonal antibody (for detection of RIG-I). Reproducibility was confirmed with additional experiments (see supplemental figures).

Construction of RIG-I 3KA and 5KA Mutant Genes—The C-terminal three or five lysine residues were mutated into alanines (designated as 3KA and 5KA). RIG-I 3KA has K888A, K907A, and K909A, whereas RIG-I 5KA has K849A, K851A,